



HAL
open science

The translational landscape of Arabidopsis mitochondria

Noelya Planchard, Pierre Bertin, Martine Quadrado, Céline Dargel-Graffin,
Isabelle Hatin, Olivier Namy, Hakim Mireau

► To cite this version:

Noelya Planchard, Pierre Bertin, Martine Quadrado, Céline Dargel-Graffin, Isabelle Hatin, et al..
The translational landscape of Arabidopsis mitochondria. *Nucleic Acids Research*, 2018, 46 (12),
pp.6218-6228. 10.1093/nar/gky489 . hal-02145349

HAL Id: hal-02145349

<https://hal.science/hal-02145349>

Submitted on 4 Jun 2019

HAL is a multi-disciplinary open access archive for the deposit and dissemination of scientific research documents, whether they are published or not. The documents may come from teaching and research institutions in France or abroad, or from public or private research centers.

L'archive ouverte pluridisciplinaire **HAL**, est destinée au dépôt et à la diffusion de documents scientifiques de niveau recherche, publiés ou non, émanant des établissements d'enseignement et de recherche français ou étrangers, des laboratoires publics ou privés.



Distributed under a Creative Commons Attribution - NonCommercial 4.0 International License

The translational landscape of *Arabidopsis* mitochondria

Noelya Planchard^{1,2,†}, Pierre Bertin^{3,†}, Martine Quadrado¹, Céline Dargel-Graffin¹,
Isabelle Hatin³, Olivier Namy^{3,*} and Hakim Mireau^{1,*}

¹Institut Jean-Pierre Bourgin, INRA, AgroParisTech, CNRS, Université Paris-Saclay, RD10, 78026 Versailles Cedex, France, ²Paris-Sud University, Université Paris-Saclay, 91405 Orsay Cedex, France and ³Institute for Integrative Biology of the Cell (I2BC), UMR 9198 CEA, CNRS, Univ. Paris Sud, Bâtiment 400, 91405 Orsay, France

Received September 22, 2017; Revised May 15, 2018; Editorial Decision May 17, 2018; Accepted May 22, 2018

ABSTRACT

Messenger RNA translation is a complex process that is still poorly understood in eukaryotic organelles like mitochondria. Growing evidence indicates though that mitochondrial translation differs from its bacterial counterpart in many key aspects. In this analysis, we have used ribosome profiling technology to generate a genome-wide snapshot view of mitochondrial translation in *Arabidopsis*. We show that, unlike in humans, most *Arabidopsis* mitochondrial ribosome footprints measure 27 and 28 bases. We also reveal that respiratory subunits encoding mRNAs show much higher ribosome association than other mitochondrial mRNAs, implying that they are translated at higher levels. Homogenous ribosome densities were generally detected within each respiratory complex except for complex V, where higher ribosome coverage corroborated with higher requirements for specific subunits. In complex I respiratory mutants, a reorganization of mitochondrial mRNAs ribosome association was detected involving increased ribosome densities for certain ribosomal protein encoding transcripts and a reduction in translation of a few complex V mRNAs. Taken together, our observations reveal that plant mitochondrial translation is a dynamic process and that translational control is important for gene expression in plant mitochondria. This study paves the way for future advances in the understanding translation in higher plant mitochondria.

INTRODUCTION

The functioning of eukaryotic cells relies on the integrated activity of several highly specialized subcellular or-

ganelles. Among them, mitochondria represent essential energy conversion powerhouses that produce most of the energy of cells through aerobic respiration. Mitochondria have an exogenous origin and the prevailing view is that they arose from the endosymbiotic acquisition of an ancient α -proteobacteria (1,2). Throughout evolution, the adoption of mitochondria has been associated with a substantial reduction in their genetic content. Modern mitochondrial genomes encode only a handful of mRNAs (33 in *Arabidopsis thaliana*) that are translated within the organelle. This requires the existence of a complete gene expression machinery whose most factors are encoded by nuclear genes. Gene expression in mitochondria therefore involves the cooperation between highly degenerated bacterial-like features inherited from the original endosymbiont and eukaryotic-derived nuclear-encoded *trans*-factors that appeared throughout evolution. This dual origin has resulted in complex mRNA expression processes involving a high number of post-transcriptional modifications (3,4). In recent years, significant progress has been made concerning certain aspects of gene expression in plant mitochondria (4). However, mitochondrial translation, the last level of mRNA expression that is also the least prone to easy molecular analyses, has remained largely unexplored in plants. Nevertheless, we know that the mitochondrial translation machinery differs profoundly from its bacterial counterpart in many essential aspects, and that the major translation-associated components are substantially different from those found in bacteria (3,5,6). In particular, the rRNA and protein composition of mitoribosomes differ extensively from those of *Escherichia coli* ribosomes (7, 8). Additionally, the constraints associated with the translation of mRNAs encoding mostly hydrophobic respiratory subunits have led to highly specialized translation mechanisms guided by membrane-associated mitochondrial ribosomes (mitoribosomes) to facilitate cotranslational insertion of mitochondria-encoded proteins into the inner mitochondrial membrane (9). The divergence with bacteria is

*To whom correspondence should be addressed. Tel: +33 130 833 070; Fax: +33 130 833 319; Email: hakim.mireau@inra.fr
Correspondence may also be addressed to Olivier Namy. Tel: +33 169 155 051; Fax: +33 169 157 296; Email: olivier.namy@i2bc.paris-saclay.fr
†The authors wish it to be known that, in their opinion, the first two authors should be regarded as Joint First Authors.

also particularly obvious for the translation initiation step since plant mitochondrial mRNAs lack the typical ribosome anchoring motifs in their 5' leaders that are used in prokaryotes to help position the start codon at the P-site of the ribosome (7). Thus, we currently do not know how mitochondrial ribosomes are recruited to 5' untranslated regions (UTR), nor how the correct translation initiation codon is recognized by the small ribosomal subunit. The high degree of sequence divergence among 5' leaders of plant mitochondrial mRNAs has suggested a ribosome recruitment mechanism involving gene-specific *cis*-sequences and trans-factors (10,11). Up until now only two proteins belonging to the large family of pentatricopeptide repeat (PPR) proteins have been shown to promote mitochondrial translation initiation in higher plants (12,13). The mechanisms by which these PPR proteins help to recruit the mitoribosome toward the AUG codon of their target mitochondrial mRNA have, however, not yet been determined. Moreover, the sequence of mitochondrial transcripts in plants is extensively modified through a process called RNA editing in which more than 400 precisely-selected cytidine residues are converted into uridines. In general, C-to-U RNA editing restores conserved codons of coding sequences and is thus essential for the proper function of mitochondrial proteins and subsequently the activity of the organelle. However, a large number of these sites are not edited to 100%, rendering plant mitochondrial mRNA sequences heterogeneous (14,15). How mitochondrial translation and RNA editing machineries functionally coordinate remains an open question. Contradictory results have been obtained with regard to a few mitochondrial transcripts (16–20), but a genome-wide view of the functional relationship between RNA editing and translation is currently lacking.

The recent development of ribosome profiling technology has greatly facilitated the detailed measurement of translation at the single-nucleotide level and on a genome-wide scale (21). Its general principle consists in the purification and subsequent sequencing of short mRNA segments covered by the translating ribosomes. These mRNA segments are called ribosome footprints and measure about 30-nt long in most species (22). The statistical analysis of their distribution reveals the identity and boundaries of translated RNA regions and provides measurements of their relative translational levels. This technology has recently revealed interesting functional aspects about ribosome behavior in plastid and human mitochondria, but had been never used to study plant mitochondrial translation (23–25). In order to gain a comprehensive view of the *Arabidopsis* mitochondrial translational machinery and the functioning of the plant mitochondrial machinery, we have prepared and sequenced total ribosome footprints from *Arabidopsis* inflorescences and mapped them to the *Arabidopsis* mitochondrial genome. Notably, this approach has allowed us to estimate and compare the translational activity among mitochondrial mRNAs, to see how mitochondrial translation is reorganized in respiratory mutants and whether edited mRNAs preferentially associate with mitochondrial polysomes.

MATERIALS AND METHODS

Plant material

Arabidopsis (*A. thaliana*) Col-0 plants were obtained from the Arabidopsis Stock Centre of Institut National de la Recherche Agronomique in Versailles (<http://dbgap.versailles.inra.fr/portail/>). *Arabidopsis mtsf1* and *mtl1* mutants were previously described (13,26). Plants were grown in a greenhouse in long day conditions for 10–12 weeks before use. Flowers were harvested simultaneously for all genotypes, snap-frozen in liquid nitrogen and stored at -80°C until use.

Ribosome footprints preparation

Total ribosome footprints were prepared from a mix of flower buds and open flowers following a procedure adapted from (23,27). About 2.5 g of flowers were ground in liquid nitrogen and resuspended in 15 ml of ribosome extraction buffer (0.2 M sucrose, 0.2 M KCl, 40 mM Tris-acetate, pH 8, 10 mM MgCl_2 , 10 mM β -mercaptoethanol, 2% polyoxyethylene 10 tridecyl ether, 1% Triton X-100, 100 $\mu\text{g/ml}$ chloramphenicol and 100 $\mu\text{g/ml}$ cycloheximide). The obtained solution was centrifuged twice for 10 min at 15 000 g at 4°C to remove the cell debris and the supernatant was transferred to a new tube. To estimate the RNA concentration contained in the supernatant, total RNA was extracted from a 0.5 ml aliquot using the TRI Reagent[®] (Sigma-Aldrich) following the manufacturer's instructions. The supernatant was then digested with 10 U/OD260nm/ml of RNase I (Ambion), and incubated 1 h at 25°C to degrade unprotected RNA. The solution was then layered on an equal volume of a sucrose cushion (1 M Sucrose, 0.1 M KCl, 40 mM Tris-acetate, pH 8, 15 mM MgCl_2 , 5 mM β -mercaptoethanol, 100 $\mu\text{g/ml}$ chloramphenicol and 100 $\mu\text{g/ml}$ cycloheximide) and centrifuged for 3 h at 55 000 g at 4°C in a TFT 65-13 rotor (Kontron). The obtained pellet was resuspended in 0.6 ml of RNA extraction buffer I (0.1 M EGTA pH 8, 0.1 M NaCl, 1% sodium dodecyl sulphate (SDS), 10 mM Tris-HCl pH 8 and 1 mM ethylenediaminetetraacetic acid (EDTA)), and RNAs were extracted with the TRI Reagent[®] (Sigma-Aldrich) following the manufacturer's recommendations. Ribosomal footprints were further purified on 17% (v/v) acrylamide-bisacrylamide (19:1) gel made with 7 M urea and 1 \times Tris-acetate-EDTA (TAE) buffer. For this, 600 μg of RNAs were electrophoresed in two separated 15 cm-wide wells. The gel was pre-run for 1 h at 50°C and then run for 15–16 h at 90 V at the same temperature. A mix comprising 100 ng of 27-mer and 33-mer RNA oligonucleotides was loaded on both gel extremities and used as size marker. After staining for 30 min in 1 \times SYBR Gold (Life Technologies) diluted in 1 \times TAE, RNA contained in the 27 and 33 nt regions were separately excised from the gel. The gels slices were stored at least 2 h at -20°C and then physically disrupted by centrifugation through a needle hole made in a 0.5 ml microcentrifuge tube nested in an outer 1.5 ml collection microtube. The tube assembly was centrifuged at maximum speed for 5 min. RNAs were eluted overnight from gel fragments by passive diffusion in 5 ml of RNA extraction buffer II (10 mM Tris-HCl pH 8, 1 mM EDTA, 0.1 M NaCl, and 0.2%

SDS) at 4°C on a rotating wheel. The recovered RNAs were then isolated with the TRI Reagent[®] (Sigma-Aldrich) following the manufacturer's instructions, resuspended in 30 µl of RNase-free water and stored at -80°C until use.

Ribosome footprints were depleted from ribosomal RNA with the Ribo-Zero Plant kit (Illumina) following manufacturer's recommendations. Sequencing libraries were prepared with the TruSeq Small RNA library preparation kit (Illumina). Next generation sequencing was performed by Beckman (single end, 50 nt).

Total RNA quantification

The abundance of mitochondrial mRNAs contained in each genotype used was determined by quantitative RT-PCR as described in (13). Primers were designed to quantify the abundance of each exon of mitochondrial mRNAs of known function, except for the *nad5* exon 3 that is too small to be quantified by quantitative RT-PCR (see Supplementary Table S1).

RNA-seq analysis

A total of 5 µg of RNA (derived from the initial step of ribosome footprint purifications) were depleted from ribosomal RNA with the Ribo-Zero Plant kit (Illumina) following manufacturer's recommendations. Sequencing libraries and next generation sequencing was performed by Beckman (single end, 50 nt).

Bioinformatic analysis

From raw data to alignment files. Raw data were first trimmed to remove the 3' adapter sequence with CutAdapt 1.9.1 (28) configured with $-e$ 0.12, $-m$ 24, $-M$ 35 and $-a$ options to select a read size in a range from 24 to 35 nt allowing 12% of error. The trimmed reads were then mapped against the rRNA sequences of *A. thaliana* (www.arabidopsis.org) with Bowtie 1.1.2 (29) set up with $-all$ and $-un$ options. The $-un$ option was used to select all unmapped reads. These filtered reads were finally mapped against the complete Col-0 mitochondrial genome (JF729201.1) or only the coding sequences with Bowtie 1.1.2. The latter alignments were configured with two mismatches allowed ($-n$ 2) and only uniquely mapped reads were selected ($-m$ 1). The sam formatted files generated by the aligner were converted to sorted and indexed bam formatted files using the Samtools program (30). All the pipeline was automatized through the use of Snakemake workflow engine version 3.5.2 (31).

Differential expression. The number of reads for each gene was calculated with featureCounts 1.5.0-p2 program (32) and normalized with DESeq2 method (33) through SAR-Tools R Package (34). Snakemake workflow engine was also used to automatize the steps of this analysis.

For the analysis of editing, we generated new alignment files by mapping the filtered reads on the non-edited Col-0 mitochondrion genome and the edited one. These alignments were done with zero mismatch allowed and selecting only uniquely mapped reads. Then, with a homemade

Python3 script, we parsed the alignment files and extracted the percentage of C and U for each mitochondrial editing position listed in (14). Using this approach, editing efficiencies were calculated from both Ribo-seq and RNA-seq sequencing data that were generated in the course of the present analysis.

The data discussed in this publication have been deposited in NCBI's Gene Expression Omnibus and are accessible through GEO Series accession number GSE104028.

Mapping of RNA-seq reads to mitochondrial mRNA extremities. Reads alignments were performed with Bowtie 1.1.2 (29).

RESULTS

Most mitochondrial ribosome footprints in *Arabidopsis* measure 27 and 28 nt

To get a comprehensive view of all ribosome-associated mRNA regions in *Arabidopsis* mitochondria, we generated total ribosome footprints and mapped the obtained reads to the *Arabidopsis* mitochondrial genome. To optimize the recovery of mitochondrial ribosome footprints from total extracts, polysomes were prepared from *Arabidopsis* flowers which are known to contain high amounts of active mitochondria (35). The presence of 1% Triton in the extraction buffer allowed us to extract both soluble and membrane-bound mitochondrial polysomes and thereby obtain good ribosome protected fragment (RPF) coverage along all mitochondrial transcripts. Since the size of selected RNA fragments from preparative gels can strongly influence the recovery of the desired ribosome footprints, we built upon a recent publication indicating that ribosome footprints in human mitochondria showed a bimodal distribution peaking at 27 and 33 nt (24). To determine whether *Arabidopsis* mitoribosome footprints measured either or both of these sizes, RNA bands at 27 and 33 bases were extracted from preparative polyacrylamide gels and sequenced. Sequence analysis of the reads mapping to the mitochondrial genome indicated that the 27-nt RNA population mostly contained fragments of 27, 28 and 29 bases, whereas the 33-nt band was essentially composed of 32, 33 and 34-base RNA fragments (Supplementary Figure S1). The strongest evidence that these fragments corresponded to ribosomal footprints was their biased repartition relative to the start codon of mitochondrial coding sequences. Indeed, ribosomes move triplet by triplet, and we were expecting to observe the same regularity for their footprints. In fact, the two RNA categories show very different behavior regarding their bias to the start codon (Figure 1). The longest fragments (32/34-mers) displayed a perfect random distribution in the three possible reading frames whereas the smallest fragments (27/29-mers) showed a clear repartition bias. We could effectively observe a bias toward the phase 2 for all the k-mers when analyzing their 3' extremities, whereas the phase bias differed for each k-mer at their 5' end. Mapping to mitochondrial genes further revealed that the 27 and 28-nt reads mapped primarily to coding sequences and to a much lesser extent to UTRs and introns (Supplementary Figure S2A). In contrast, the 32/34-mers mapped mostly to

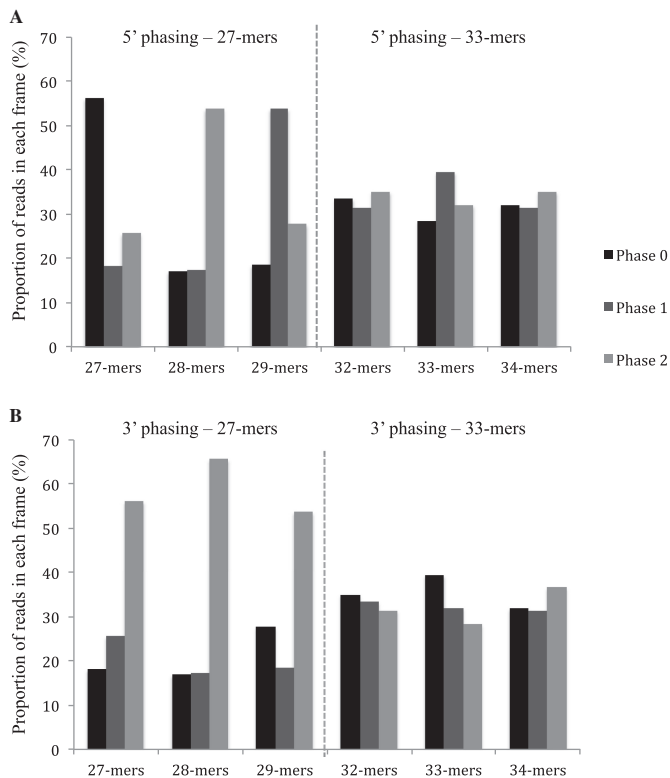


Figure 1. The 27-nt RPF population shows a better periodicity relative to mitochondrial gene start codons compared to the 33-nt RNA population. (A) 5' phasing of the 27-mer and 33-mer populations. (B) 3' phasing of the 27-mer and 33-mer populations.

the 5'UTRs of genes and much less frequently to mitochondrial coding sequences (Supplementary Figure S2B). Overall, this preliminary analysis showed us that the majority of *Arabidopsis* mitochondrial ribosome footprints are 27–29 nt long, and that those with 32–34 nt contribute very poorly to the mitoribosome footprint population. Consequently, all our subsequent analyses were done after recovery of the 27–29 nt RNA band from preparative gels.

Analysis of ribosome footprint distributions along mitochondrial genes sequences

A first global analysis of the distribution of *Arabidopsis* mitochondrial RPF was done from a total of 900 million high quality reads obtained from wild-type plants. Less than 2% (1.9%) of these reads could be aligned to the mitochondrial genome of the Col-0 accession (JF729201.1) and 38% to the nuclear and plastid genomes, indicating that mitochondrial ribosome footprints represent a mere fraction of total ribosome footprints generated from flowers. The vast majority of reads aligned with exons corresponding to known mitochondrial genes, further supporting that they were indeed mitochondrial ribosome footprints. Despite its relative small size, the *Arabidopsis* mitochondrial genome contains a large number of duplicated regions, preventing the correct mapping of RPF along the entire sequence. This was particularly obvious for *atp6-1* and *atp6-2* genes that share identical 3' regions. The partial overlap be-

tween the *rps3* and *rpl16* genes was also problematic in this respect. Despite these classical limitations, the alignments obtained allowed us firstly to examine the translation initiation and termination sites of genes of known function. For most genes, the ribosome footprint distributions were coherent with the proposed positions of start and stop codons (<http://www.arabidopsis.org/>). We focused on the few mitochondrial transcripts for which the translational initiation and termination codons were shown to be removed by post-transcriptional mRNA processing. This concerns the *rps4* mRNA that has been shown to be processed two bases downstream of its AUG and the *nad6*, *mttB* and *ccmC* mRNAs that are matured 17, 10 and 46 nt upstream of their annotated stop codon, respectively (36,37). We first used the RNA-seq data we obtained from Col-0 plants to check these transcript extremities. This allowed us to unambiguously confirm that the vast majority *rps4* transcripts are effectively devoid of any AUG (Figure 2A) and that *nad6* and *ccmC* mRNAs do not carry any translational stop codon (Figure 2B). The situation is more mitigated for *mttB*, however most *mttB* mRNAs lack any translational termination codon. In agreement with these truncated mRNA ends, we observed that the ribosome footprints on *rps4* initiate 14 bases downstream of the annotated AUG (Figure 2A). Similarly, the RPF distributions along *nad6* and *ccmC* terminate a few bases upstream of their mapped 3' extremity and do not extend until the predicted stop codon (Figure 2B). No ribosome footprints was found to cover the annotated stop codon of *mttB* and the presence of a high RPF peak just upstream suggest a ribosome pausing site resulting from the post-transcriptional removal of the terminal UGA. Altogether, these observations suggest that the translation initiation and termination in plants show surprising flexibility and that the plant translational machinery evolved ways to efficiently decode mRNAs devoid of conventional AUG or STOP codons.

To potentially identify new coding regions within the mitochondrial genome, we also searched for RPF signals located outside of annotated regions. We looked for regions of at least 100 bases long, comprising a minimum of 10 ribosome footprints overall and in which 70% of the nucleotides are covered by at least 1 RPF. The 5' and 3' extremities of these regions were defined when a minimum of 40 nt with no RPF was encountered. Using these criteria, no signal outside of known genes could be identified, therefore, our approach did not reveal any new translated protein-coding ORFs in *Arabidopsis* mitochondria.

Arabidopsis mitochondrial mRNAs show highly different ribosome association levels and ribosome entry mechanisms

To estimate and compare the translational efficiencies of *Arabidopsis* mitochondrial mRNAs, we determined the relative density of ribosome footprints per gene. To allow comparison between genes, the calculated densities were normalized to both transcript length and abundance. This approach revealed clear differences in ribosome density between mRNAs (Figure 3). Globally, mRNAs encoding respiratory chain subunits showed much higher ribosome loading levels compared to other mitochondrial transcripts, implying a greater translational activity for these genes.

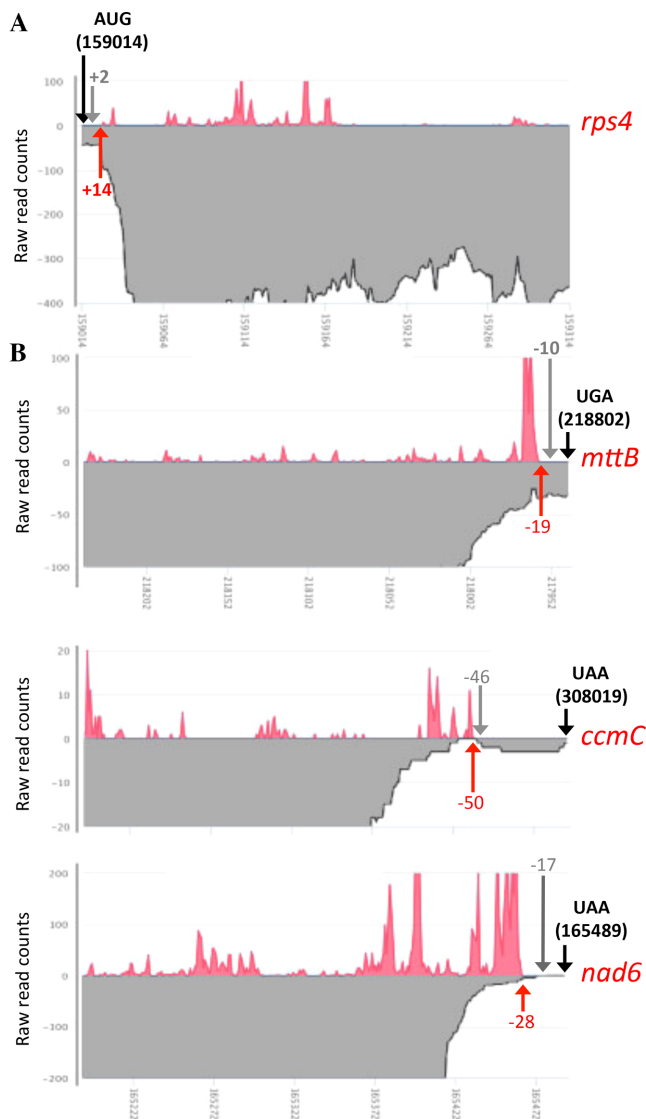


Figure 2. Ribosome footprint densities near the extremities of *Arabidopsis* mitochondrial mRNAs for which the start or the stop codons are removed by post-transcriptional processing. Ribosome footprint distributions are shown as red curves and RNA-seq read densities are depicted in gray. (A) Close-up view showing the first 300 nt of the *rps4* mRNA. (B) Close-up view showing the last 300 nt of the *nad6*, *mttB* and *ccmC* mRNAs. Black arrows materialize the positions of the theoretical translation start or stop codons and their coordinate on the mitochondrial genome of Col-0 is specified. Red arrows and the associated numbers indicate the start (*rps4*) or the end (*nad6*, *mttB* and *ccmC*) of observed Ribo-seq signals, respectively to either the translational start or stop codon of each transcript. Gray arrows and the associated numbers indicate the position of the 5' (*rps4*) or 3' (*nad6*, *mttB* and *ccmC*) mRNA extremities mapped by circular RT-PCR in (36,37).

Within each respiratory complex, small differences in translational efficiencies were observed except for the ATP synthase complex (V). The *atp1*, *atp4*, *atp8* and mostly *atp9* showed significantly higher ribosome densities compared to *atp6-1* and *atp6-2*. Interestingly, the two copies of the *atp6* gene also appear to be translated at different levels, and the *atp6-1* gene showed much higher ribosome density compared to *atp6-2* (Figure 3 and Supplementary Figure

S3). All other mitochondrial genes, notably the ones coding for c-type cytochrome maturation and ribosomal proteins, had particularly low ribosome loading densities along their transcripts suggesting that they are translated at low levels. Low levels of ribosome footprints were also detected for the *matR* and *mttB* coding sequences, supporting the proposed functionality of these two genes (38,39).

The relative distributions of ribosome footprints along the five di-cistronic mitochondrial transcripts (37) showed different patterns, implying different mechanisms to guide the ribosomes toward the downstream cistrons. Regarding the *nad4L-atp4* (3300 reads per kilobase million (RPKM)) for *nad4L* versus 4500 for *atp4*) and *rpl5-cob* (1150 versus 4600 RPKM) transcripts, the ribosome density in the downstream open reading frame appeared to be higher compared to the upstream open reading frame (Supplementary Figure S4). An internal entry of mitoribosomes just upstream of the translation start codon of the downstream cistron in these two cases may explain this increase. The translation of *rps3-rpl16* also implies independent entry of mitoribosomes, as the two orfs overlap and are encoded on different reading frames. Conversely, the ribosome density along the downstream open reading frame was much lower in the case of the *nad3-rps12* mRNA (4900 versus 450 RPKM), suggesting a less efficient translation of *rps12* (Supplementary Figure S4). This could be explained either by an inefficient internal entry of ribosomes upstream of *rps12* or by a weak re-initiation downstream of *nad3*.

The translation of mitochondrial mRNAs is not dependent on their editing status

The C-to-U RNA editing process corrects more than 400 positions in plant mitochondrial transcripts (14,15). Most editing events reestablish a correct identity to codons so that edited mRNAs encode functionally optimal mitochondrial proteins (15). Nevertheless, many mitochondrial sites are not edited to 100% and a large proportion of plant mitochondrial mRNAs can encode potentially sub-optimal, if not inactive, proteins. To see whether the plant mitochondrial translation machinery preferentially associates with fully edited transcripts or not, we evaluated the editing status of transcripts associated with *Arabidopsis* mitochondrial ribosomes. We calculated the editing levels of all known mitochondrial RNA editing sites from both total and ribosome-associated RNAs (Supplementary Table S2). Of the 434 previously identified editing sites (14), 81 appeared to be covered by less than 10 ribosome footprints and were therefore excluded from further analysis because of insufficient coverage. Among the 353 remaining sites, most partially edited sites remained partially edited in polysome-associated mRNAs, revealing at the level of the entire mitochondrial transcriptome that complete editing of mitochondrial mRNAs is not an absolute prerequisite for their translation. A slight increase in C-to-U transition efficiencies could, however, be detected at many positions in polysomal mRNAs. In effect, we observed that 70% of sites (58 out of 80) whose editing levels range between 10 and 90% showed increased editing levels when contained in mitoribosome-associated mRNAs compared to total mRNAs (Figure 4A). The editing increase for these more-edited

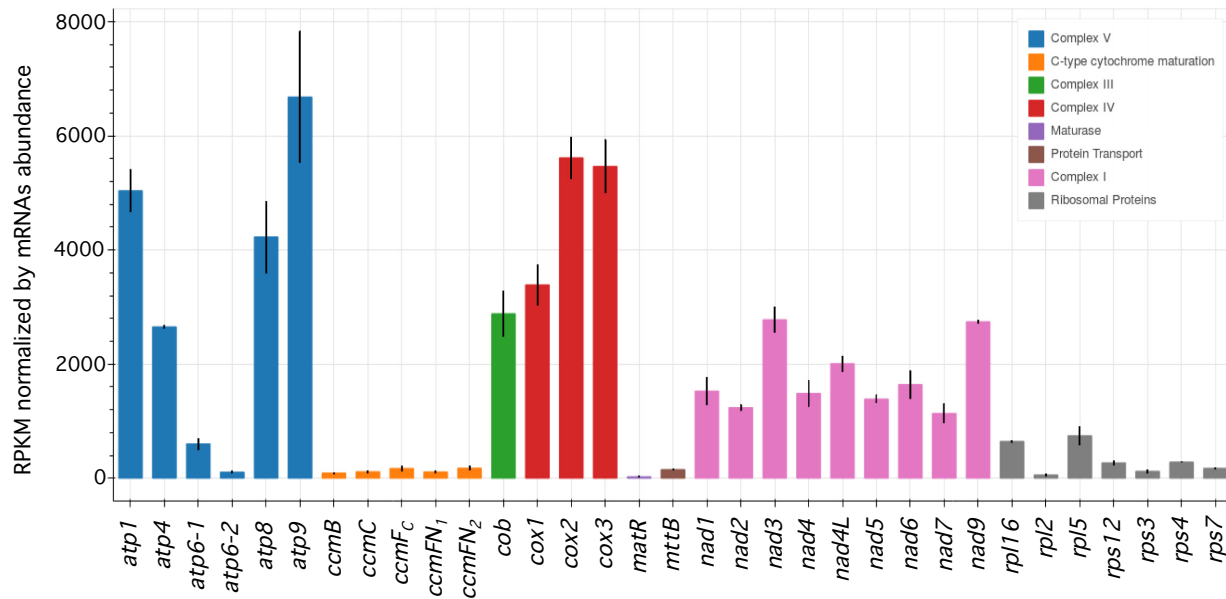


Figure 3. Protein-coding mitochondrial mRNAs show large differences in ribosome footprint densities in *Arabidopsis*. RPF densities normalized to both mRNA length and abundance are shown. Mitochondrial mRNAs are indicated and color-coded according to the respiratory complex or the functional category to which they belong. Means \pm SE ($n = 2$).

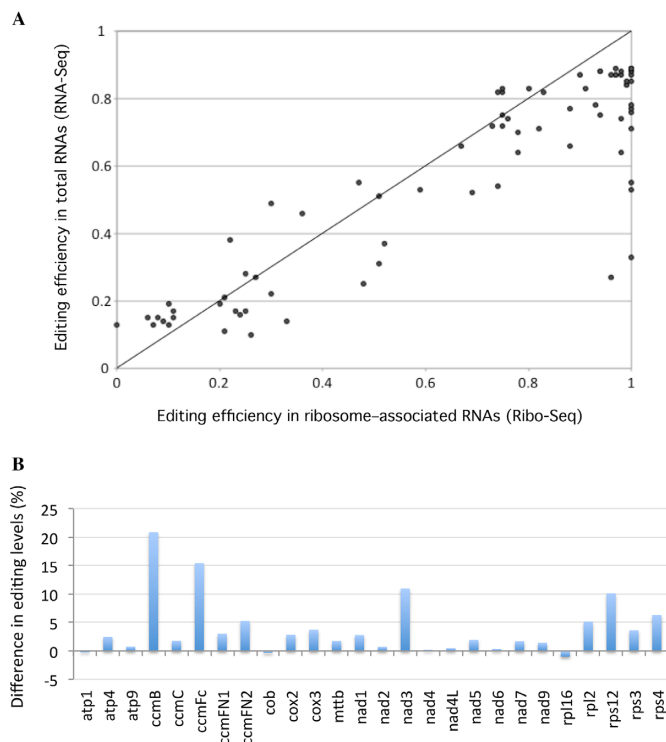


Figure 4. Mitochondria-encoded mRNAs are more edited when they associate with mitoribosomes. (A) C-to-U editing levels calculated from total (RNA-seq) and ribosome-associated (Ribo-seq) RNA populations are presented. To identify potential variations in editing efficiencies, only sites that are partially edited and whose editing efficiencies is comprised between 10 and 90% in total RNAs were considered in the analysis. (B) Average editing levels of mitochondrial mRNAs were determined from both ribosome footprint and total RNA populations. The differences of editing levels calculated from both RNA samples (polysomal RNA—total RNA) are shown.

sites is around 16% overall and most of them are distributed in different mitochondrial transcripts (Figure 4B). Nevertheless, quite a few are contained in *ccmB*, *ccmFc*, *nad3* and *rps12* RNAs, whose global editing levels are much higher in ribosome-protected RNAs compared to total RNAs (Figure 4B). Most of the sites whose editing levels reach almost 100% when associated with ribosomes are contained in these four mitochondrial transcripts.

Mitochondrial translation is reorchestrated in respiratory complex I mutants

To better understand the plasticity of mitochondrial translation and the extent to which it participates in regulating gene expression in the organelle, we determined mitochondrial translational changes in two complex I respiratory mutants. For this approach, we chose the *mtl1* and *mtsfl* mutants, which are two *ppr* mutants affected in the translation of *nad7* mRNA and in the stability of *nad4* transcript respectively (13,26). These two mutants show different growth retardation phenotypes, with *mtsfl* plants being much more impaired in their development than the *mtl1* plants. In both mutants, the ribosome densities and the steady state levels of mitochondrial mRNAs were quantified. In response to the lack of respiratory complex I, we observed a global over-accumulation of most mitochondrial transcripts in both mutants (Supplementary Figure S5). The increase in transcript abundance varied among genes and was comprised between 1.5- and 4.5-folds. Interestingly, this change did not correlate with an equivalent increase in ribosome density for most transcripts. Effectively, many mRNA species showing higher abundance contained either similar or even lower ribosome loading compared to the wild-type, suggesting that mitochondrial translation is a tightly regulated process that does not simply follow the changes in transcript abundance

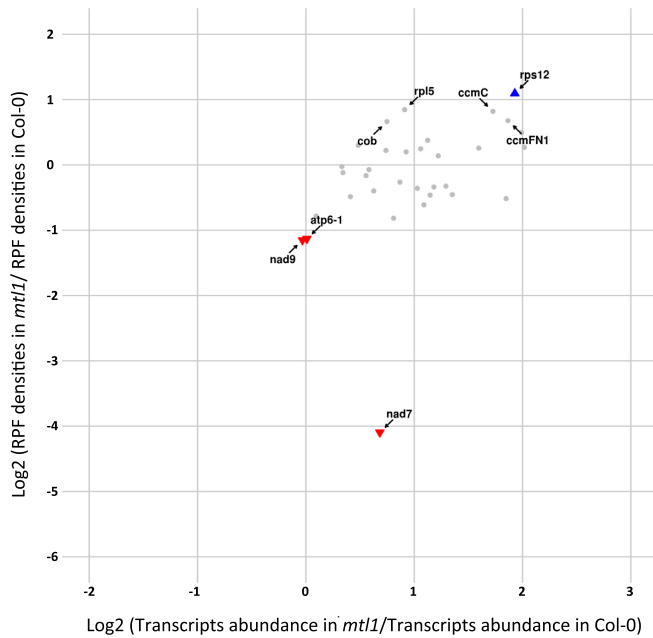


Figure 5. Differential transcriptional and translational profiles of mitochondria-encoded mRNAs in *mtl1* and wild-type plants. For each mitochondrial mRNA, relative RPF densities (Y-axis) and transcript abundance (X-axis) are reported. Genes whose names are indicated show significant changes in ribosome occupancies compared to the wild-type (P -value < 0.05). Colored triangles show genes whose changes in ribosome loads are larger than 2-fold compared to wild-type plants.

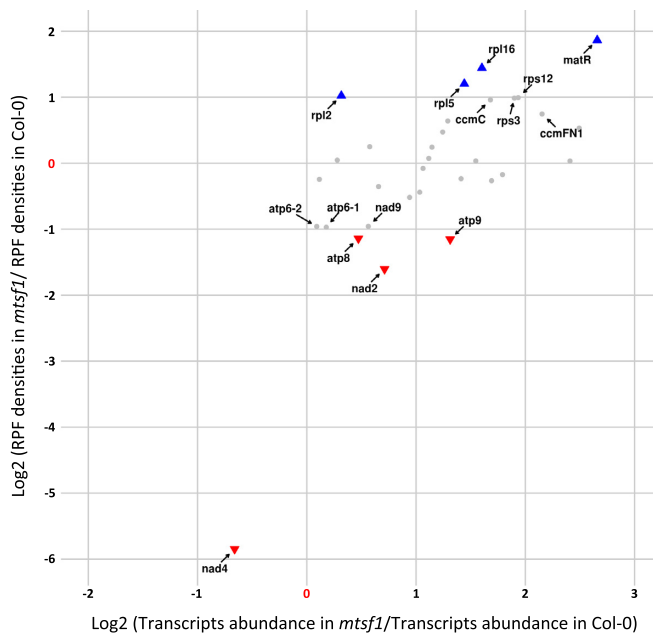


Figure 6. Differential transcriptional and translational profiles of mitochondria-encoded mRNAs in *mts1* and wild-type plants. For each mitochondrial mRNA, relative RPF densities (Y-axis) and transcript abundance (X-axis) are reported. Genes whose names are indicated show significant changes in ribosome occupancies compared to the wild-type (P -value < 0.05). Colored triangles show genes whose changes in ribosome loads are larger than 2-fold compared to wild-type plants.

(Figures 5 and 6; Supplementary Figures S6 and 7). Other-

wise, the major transcript expression defects that are known to occur in *mtl1* and *mts1* mutants were confirmed by our analysis. Regarding *mtl1*, our ribosome profiling data confirmed the strong and specific reduction of *nad7* mRNA translation despite a 1.7-time over-accumulation of its transcript (Figure 5 and Supplementary Figures S6). A strong reduction in the association of ribosomes with *nad4* mRNA was detected in *mts1* (Figure 6 and Supplementary Figures S7), which correlated with the strong destabilization of the *nad4* transcript, excluding a role of MTSF1 in *nad4* translation. For other transcripts, the comparison of *mts1* and *mtl1* translation profiles identified differences, but interesting overlaps were also observed. Among mRNAs whose translation varied most significantly in both mutants (P -value < 0.05 and $RP \log_2(FC) \geq$ or ≤ 1) several corresponded to ribosomal protein genes. Of the seven genes showing increased ribosome occupancy in *mts1* compared to the wild-type, five corresponded to ribosomal protein mRNAs, namely *rps3*, *rps12*, *rpl2*, *rpl5* and *rpl16* (Figure 6). In the *mtl1* mutant, *rps12* and *rpl5* transcripts also showed significant increases in ribosome loading in comparison to the wild-type (Figure 5). The translation of the *nad9* transcript also appeared to vary in a similar manner in both mutants. An ~ 2 -fold decrease in *nad9* translation was measured in both mutants, whereas the abundance of *nad9* transcripts remained the same in *mtl1* and was slightly increased in *mts1* compared to the wild-type (Figures 5 and 6; Supplementary Figure S5). Interestingly, moderate but significant reductions in ribosome loading on several F_1F_0 -ATP synthase transcripts were also detected in both mutants. This concerned the *atp8*, *atp9*, *atp6-1* and *atp6-2* transcripts in *mts1* plants and the *atp6-1* transcript in *mtl1* plants (Figures 5 and 6).

DISCUSSION

Unlike in human and yeast mitochondria, *Arabidopsis* mitoribosome footprints measure 27–29 nt long

Messenger RNA translation is a complex multi-step process that is still poorly understood at the molecular level in genome-containing organelles like mitochondria. Growing evidence indicates that although these organelle are of prokaryotic origin, mitochondrial translation has significantly diverged from its bacterial counterpart. Additionally, mitochondrial translation displays considerable species-specific specialization that evolved to adapt translation requirements to mitochondrial genome organization (40). These adaptations are exemplified by the variable composition and structure of mitoribosomes that differ not only between species, but also from modern bacterial ribosomes (41–43). In this analysis, we have used ribosome profiling technology to generate a genome-wide snapshot of mitochondrial translation in *Arabidopsis*, and obtained the first global analysis of a plant mitochondrial transcriptome. This approach revealed that *Arabidopsis* mitochondrial ribosome footprints measure mainly 27 and 28 nt in length and thereby do not seem to follow a bimodal distribution peaking at 27 and 33 nt as previously found for human mitochondria (24). In effect, the 27 and 28 nt RPFs presented a frame-specific distribution whereas those of 33 bases did not

show any periodicity with respect to the start codons of mitochondrial genes (Figure 1). Additionally, the 27 and 28 nt RPFs aligned to translationally active mitochondrial coding sequences (Supplementary Figure S2A), as shown by the lack of coverage of *nad7* mRNA in the *mtl1* mutant that is specifically deficient in the translation of this transcript (Supplementary Figure S8; (13)). In contrast, the 33-nt RNA population aligned poorly with *Arabidopsis* mitochondrial coding sequences (Supplementary Figure S2B) and was accordingly found to represent a very minor fraction of mitoribosome-protected fragments in maize (25). Thus, these fragments make only a modest contribution to the mitoribosome footprint population in *Arabidopsis*. Interestingly, a recent study indicated that mitoribosome footprints in yeast measure around 38 nt (44). Fragments of this size are almost inexistent in the maize mitoribosome RPF population (25) and do not appear, therefore, to be major representatives of mitoribosome footprints in plants. The discrepancy between human, yeast and *Arabidopsis* regarding the size distribution of mitochondrial RPFs is currently unclear, but may result from differences in sample preparation or in mitoribosome structures between plants, yeast and animals (24).

A global alignment to the mitochondrial genome showed that mitochondrial RPFs are distributed over all the open reading frames of most genes of known function. For mRNAs like *rps4*, *ccmC*, *nad6* or *mttB* for which the start or the stop codons are removed post-transcriptionally the RPF distributions coincide with their mapped 5' or the 3' extremities (Figure 2), confirming that despite the truncations in their coding sequence these transcripts are still competent for translation. Indeed, our RNA-seq data revealed that *ccmC*, *nad6* and *mttB* mRNAs bear highly heterogeneous 3' extremities and that most transcripts contain more or less extensive deletions at the end of the coding sequence (Figure 2B). The RPF distributions suggest that production of full-length CcmC and Nad6 proteins relies on the translation of the longest transcript forms that, nonetheless, lack any stop codon (37). Together, these observations raise questions about the mechanisms guiding mitoribosomes toward translation initiation sites in plants and also how they are released from 3'-truncated transcripts lacking stop codons such as *ccmC* or *nad6*. As suggested in mammalian mitochondria, specialized translational release factors or peptidyl hydrolases could intervene to release plant mitoribosomes stalled at the 3' extremity of mRNAs lacking stop codons (45). Several lines of evidence also support that translation initiation in plant mitochondria is a relaxed process with mitoribosomes accommodating different kinds of non-AUG start codons or initiating translation internally in di-cistronic mRNAs as suggested for *nad4L-atp4*, *rpl5-cob* and *rps3-rpl16* (Supplementary Figure S4). Accordingly, we find that mitochondrial orfs like *ccmF_{N2}*, *mttB* and *matR* that do not start with a classical AUG codon (37) are actively translated by mitoribosomes (Figure 3). Almost nothing is known about translation initiation and termination in plant mitochondria and major genetic and biochemical analyses will be required to shed light on the behavior of plant mitoribosomes.

Arabidopsis mitochondrial mRNAs are translated to highly different levels

The number of RPFs per gene, normalized by both transcript size and steady-state abundance, was used as a proxy to estimate the translational level of each mitochondria-encoded *Arabidopsis* mRNA. Assuming that the average of translation elongation rates are similar for all mitochondrial genes, this approach revealed large differences in ribosome coverage between mitochondrial protein-coding transcripts. We effectively observed that respiratory subunit mRNAs show much higher ribosome association than other types of mRNAs, notably those coding for ribosomal and c-type cytochrome maturation proteins, which appear to be translated at very low levels from our analysis (Figure 3). These results are coherent with recent quantification of plant mitochondrial proteomes which indicated that steady-state levels of respiratory chain proteins are abundant and well represented in mitochondrial proteome lists, whereas proteins of the genetic apparatus are much less abundant (46,47). The c-type cytochrome maturation proteins, the MttB transporter or the MatR maturase are present at such low levels in mitochondria that they are generally not detected at all in plant mitochondrial proteomes. The high sensitivity of the ribosome profiling technology allowed us to detect the translational activity of these very poorly translated mitochondrial mRNAs, strongly supporting their functionality. Among respiratory complexes subunits, we observed very similar ribosome densities for genes encoding proteins belonging to the same complex, except for the F₁F₀-ATP synthase. Large differences were detected between complex V mRNAs, particularly for the *atp1*, *atp4*, *atp8* and *atp9* transcripts, which showed higher RPF coverage than other *atp* mRNAs (Figure 3). The *atp1* and *atp9* mRNAs encode the α and β subunits of the F₁F₀-ATP synthase, respectively, and are present at 10 and 3 copies in complex V. The higher ribosome densities of these two transcripts, therefore, correlates with their relative stoichiometry in complex V, corroborating the proportional translation of the different ATP synthase subunits previously described in *E. coli* (48). Conversely, the higher translational activity of *atp8* compared to other single-copy complex V subunits (*atp4* and *atp6*) cannot be explained by its higher stoichiometry in the F₁F₀-ATP synthase, but suggest higher requirements for this specific subunit for reasons that need to be clarified. Interestingly, we also observed a large difference in mitoribosome coverage between the two copies of *atp6* encoded in the *Arabidopsis* mitochondrial genomes, with *atp6-1* being translated significantly more than *atp6-2* (Supplementary Figure S3). The two genes show small sequence variations in their 5' UTRs, which likely account for their differential association with mitoribosomes. Together, the large differences in ribosome densities between the various mitochondrial mRNAs reveal that translational control is an important component of gene expression in plant mitochondria. How this control operates at the molecular level is currently unclear, as we still do not know how ribosomes are recruited to mitochondrial mRNAs in the absence of Shine and Dalgarno (SD) sequences in their 5' UTR (7). This control can operate at the level of translation initiation, which is often pro-

posed as being the most rate-limiting step of translation in most systems (49,50). The combinatorial action of *cis*-acting elements within the 5'UTRs and gene-specific *trans*-factors may be responsible for the differential recruitment of ribosomes on mitochondrial mRNAs. Nonetheless, to date very few translational activators have been found to operate in plant mitochondria (12,13,51–53) and the way by which they control translation of their cognate mRNA target remains to be determined. In bacteria, SD-like sequences within coding sequences were shown to impact translation elongation and to have a major effect on mRNA translation rates (54,55). The lack of anti-SD sequence at the 3' end of the mitochondrial SSU rRNA strongly suggests that this mechanism cannot account for the differential translation of *Arabidopsis* mitochondrial mRNAs. Much remains to be discovered, therefore, before we understand how mitochondrial translation is regulated in plant mitochondria.

Mitoribosome-associated mRNAs are more edited than in total RNAs

Mitochondrial mRNAs from land plants undergo hundreds of specific C-to-U changes by RNA editing (15). In the present analysis, of the 353 *Arabidopsis* editing sites for which we obtained more than 10 reads per sites in both RNAseq and Riboseq data, 80 showed partial editing with C-to-U changes comprised between 10 and 90%. The accessibility of non-edited or partially edited mitochondrial mRNAs by the mitochondrial translation machinery has long remained an intriguing question. The translation of non-edited mitochondrial mRNA was previously suggested in a few specific cases (16–20), but no genome-wide view was available to date. By comparing C-to-U transition efficiencies in total and ribosome-associated mRNAs we observed that most partially edited sites remained incompletely edited in polysomal mRNAs confirming at a genome-wide level that complete editing of mitochondrial mRNAs is not an absolute pre-requisite for their translation (Figure 4A). Nonetheless, around 70% of these sites showed, on average, a 16% increase in their editing levels when loaded on mitoribosomes (Figure 4A and B). The origin of this increase is currently unclear, as no obvious inter-functionality between the mitochondrial translational and editing machineries has yet been revealed. As indicated, large differences in C-to-U transition efficiencies are consistently observed between editing sites in plant mitochondria (14). These differences likely result from variable functional constraints between sites, making some of them less efficiently recognized and/or processed by the editing machinery than others. Maybe, the accessibility of RNA editing sites to the editosome complex is increased when mRNAs are being translated, generating the rather global raise in editing efficiency that we observed in our riboseq data. In particular, the strong RNA helicase activity of translating ribosomes may be responsible for rendering editing sites more accessible to the editing machinery. Even with this increase, our results indicate that partially edited mRNAs are decoded by mitoribosomes, confirming at the level of the entire mitochondrial transcriptome that transcript recruitment by mitochondrial polysomes does not *a priori* discriminate between unedited and edited RNAs. A proportion

of mitochondrial polypeptides derives thus from the translation of unedited mRNAs, making 'unedited' proteins a non-negligible part of plant mitochondrial proteomes. Post-translational processes must therefore be at play to limit any potential negative effects of these likely sub-optimal 'unedited' polypeptides.

Mitochondrial translation is reorganized in *Arabidopsis* complex I mutants

The regulation of mitochondrial gene expression is fundamental not only to ensure proportional synthesis of both mitochondria and nuclear-encoded subunits belonging to the same complexes but also to adapt mitochondrial activity to the changing requirements of plants throughout their life cycle or in response to environmental stimuli. The basis of this regulation is not well understood, however several lines of evidence support that most of the control is exerted at the post-transcriptional and/or at the post-translational levels (5,56–58). To better understand to what extent mitochondrial translation participates in these regulatory circuits and gain hints about its plasticity, we measured mitochondrial translational and transcriptional changes in two contrasted complex I *Arabidopsis* mutants that accumulate either no complex I (*mtl1*) or a truncated version of it (*mtsfl*). Although both mutants have strong delays in their development compared to wild-type, the growth defects exhibited by the *mtsfl* mutant were more severe than those of *mtl1* (13,26). First, in response to complex I deficiency, we observed a 2- to 5-fold over-accumulation of most mitochondrial transcripts in mutants compared to wild-type (Supplementary Figure S5). Nonetheless, this increase in transcript abundance was not associated with an equivalent rise in ribosome coverage along mitochondrial mRNAs (Figures 5 and 6). Our analysis thus revealed that mitochondrial translation is a precisely regulated process that does not simply follow the changes in transcript abundance and that a transcript-specific translational control clearly operates in plant mitochondria. Significant changes in ribosome loading for several transcripts were, however, detected in the mutants. The most important translational change concerned the strong decrease in *nad7* ribosome occupancy in *mtl1*, confirming previously published data for this mutant (13). The impact on other mitochondrial genes was less pronounced, although some interesting tendencies were uncovered. The first one concerned the 2-fold decrease in *nad9* translation in both mutants, suggesting that the lack of functional complex I may induce a negative feedback control on the translation of this specific mRNA. As we did not detect any significant decrease in the ribosome loading of other complex I mRNAs, this means that complex I deficiency does not induce a global down-regulation of all *nad* gene translation. Interestingly, and despite a significant rise in transcript abundance, the translation of several mRNAs encoding ATP synthase subunits was lower in both complex I mutants. This negative translational control impacted a few more *atp* genes in *mtsfl* than in *mtl1* (Figures 5 and 6) and may, therefore, be correlated with the gravity of developmental alterations associated with complex I deficiency. It has recently been demonstrated that complex I-lacking *Arabidopsis* mutants compensate for the deficit in

ATP production derived from the respiratory chain by inducing higher metabolic fluxes through glycolysis and the tricarboxylic acid cycle (59). Our analysis thus reveals that these increased metabolic fluxes correlate with a slight reduction in the translation of mitochondria-encoded ATP synthase subunits. Whether or not this reduction results from a negative feedback loop induced by the reduced activity of the respiratory chain in complex I mutants remains to be clarified. Interestingly, we also observed higher ribosome association with several ribosomal protein encoding mRNAs in both *mtsfl* and *mtll* mutants. The ribosome densities of four ribosomal protein mRNA transcripts in *mtsfl* (*rps12*, *rpl2*, *rpl5*, *rpl16*) and two in *mtll* (*rps12*, *rpl5*) appeared to be increased compared to the wild-type. These observations corroborate nicely recent analyses showing that reducing the production of a mitochondria-targeted ribosomal protein resulted in an altered translation pattern in *Arabidopsis* mitochondria (60). In this mutant context, ribosomal proteins were translated more efficiently at the expense of respiratory chain encoding mRNAs. Our results suggest that an analogous reorganization of mitochondrial translational occurs in respiratory mutants, further demonstrating that plant mitoribosomes do not translate mRNAs non-selectively, but that a certain level of translational control likely operates in plant mitochondria.

Concluding remarks

Using ribosome profiling technology, we have generated a genome-wide snapshot of mitochondrial translation in *Arabidopsis* and monitored certain aspects of its dynamics. We show that mitochondria-encoded mRNAs are differentially translated and that proportional translation levels correlate with the stoichiometry of respiratory chain subunits, in particular for complex V. Moreover, a slight reorganization of mitochondrial translation could be detected in complex I respiratory mutants involving a reduction in ribosome densities for F_1F_0 -ATP synthase mRNAs and an increase in the translation of several ribosomal protein encoding transcripts. We thus reveal that mitochondrial translation is controlled at the level of individual mRNAs and that it participates in regulating the activity of plant mitochondria. Our analysis also reveals that translation of mitochondria-encoded transcripts can be satisfactorily measured from total ribosome footprint extracts and does not necessarily require the purification of mitochondria.

DATA AVAILABILITY

The data have been deposited in NCBI's Gene Expression Omnibus and are accessible through GEO Series accession number GSE104028.

SUPPLEMENTARY DATA

[Supplementary Data](#) are available at NAR Online.

FUNDING

Institut National de la Recherche Agronomique (INRA) [UMR 1318]; French Ministère de l'Enseignement et de

la Recherche and Fondation pour la Recherche Médicale [FDT20160736470 to N.P.]; LabEx Saclay Plant Sciences-SPS [ANR-10-LABX-0040-SPS]; INCa [RiboTEM 2014-092]; ANR [Rescue_Ribosome ANR-17-CE12-0024-01 to O.N.], Funding for open access charge: IJPB; INRA [UMR 1318].

Conflict of interest statement. None declared.

REFERENCES

- Gray, M.W. (1999) Mitochondrial evolution. *Science*, **283**, 1476–1481.
- Gray, M.W. (2012) Mitochondrial evolution. *Cold Spring Harb. Perspect. Biol.*, **4**, a011403.
- Lightowlers, R.N., Rozanska, A. and Chrzanowska-Lightowlers, Z.M. (2014) Mitochondrial protein synthesis: figuring the fundamentals, complexities and complications, of mammalian mitochondrial translation. *FEBS Lett.*, **588**, 2496–2503.
- Hammani, K. and Giegé, P. (2014) RNA metabolism in plant mitochondria. *Trends Plant Sci.*, **19**, 380–389.
- Janska, H. and Kwasiak, M. (2014) Mitoribosomal regulation of OXPHOS biogenesis in plants. *Front. Plant Sci.*, **5**, 79.
- Ott, M., Amunts, A. and Brown, A. (2015) Organization and regulation of mitochondrial protein synthesis. *Annu. Rev. Biochem.*, **85**, 77–101.
- Bonen, L. (2004) Translational Machinery in Plant Organelles. In: Daniell, H. and Chase, C.D. (eds) *Molecular Biology and Biotechnology of Plant Organelles*. Springer, Dordrecht, pp. 323–345.
- Greber, B.J. and Ban, N. (2016) Structure and function of the mitochondrial ribosome. *Annu. Rev. Biochem.*, **85**, 103–132.
- Pfeffer, S., Woellhaf, M.W., Herrmann, J.M. and Forster, F. (2015) Organization of the mitochondrial translation machinery studied in situ by cryoelectron tomography. *Nat. Commun.*, **6**, 1–8.
- Hazle, T. and Bonen, L. (2007) Comparative analysis of sequences preceding protein-coding mitochondrial genes in flowering plants. *Mol. Biol. Evol.*, **24**, 1101–1112.
- Choi, B., Acero, M.M. and Bonen, L. (2012) Mapping of wheat mitochondrial mRNA termini and comparison with breakpoints in DNA homology among plants. *Plant Mol. Biol.*, **80**, 539–552.
- Manavski, N., Guyon, V., Meurer, J., Wienand, U. and Bretschneider, R. (2012) An essential pentatricopeptide repeat protein facilitates 5' maturation and translation initiation of rps3 mRNA in maize mitochondria. *Plant Cell*, **24**, 3087–3105.
- Haïli, N., Planchard, N., Arnal, N., Quadrado, M., Vrielynck, N., Dahan, J., Francs-Small des, C.C. and Mireau, H. (2016) The MTL1 pentatricopeptide repeat protein is required for both translation and splicing of the mitochondrial NADH DEHYDROGENASE SUBUNIT7 mRNA in Arabidopsis. *Plant Physiol.*, **170**, 354–366.
- Bentolila, S., Oh, J., HANSON, M.R. and Bukowski, R. (2013) Comprehensive high-resolution analysis of the role of an arabidopsis gene family in RNA editing. *PLoS Genet.*, **9**, e1003584.
- Takenaka, M., Zehrmann, A., Verbitskiy, D., Härtel, B. and Brennicke, A. (2013) RNA Editing in plants and its evolution. *Annu. Rev. Genet.*, **47**, 335–352.
- Lu, B. and Hanson, M.R. (1996) Fully edited and partially edited nad9 transcripts differ in size and both are associated with polysomes in potato mitochondria. *Nucleic Acids Res.*, **24**, 1369–1374.
- Lu, B., Wilson, R.K., Phreaner, C.G., Mulligan, R.M. and Hanson, M.R. (1996) Protein polymorphism generated by differential RNA editing of a plant mitochondrial rps12 gene. *Mol. Cell. Biol.*, **16**, 1543–1549.
- Lu, B. and Hanson, M.R. (1994) A single homogeneous form of ATP6 protein accumulates in petunia mitochondria despite the presence of differentially edited atp6 transcripts. *Plant Cell*, **6**, 1955–1968.
- Phreaner, C.G., Williams, M.A. and Mulligan, R.M. (1996) Incomplete editing of rps12 transcripts results in the synthesis of polymorphic polypeptides in plant mitochondria. *Plant Cell*, **8**, 107–117.
- Williams, M.A., Tallakson, W.A., Phreaner, C.G. and Mulligan, R.M. (1998) Editing and translation of ribosomal protein S13 transcripts: unedited translation products are not detectable in maize mitochondria. *Curr. Genet.*, **34**, 221–226.
- Ingolia, N.T., Ghaemmaghami, S., Newman, J.R.S. and Weissman, J.S. (2009) Genome-wide analysis in vivo of translation with nucleotide resolution using ribosome profiling. *Science*, **324**, 218–223.

22. Brar, G.A. and Weissman, J.S. (2015) Ribosome profiling reveals the what, when, where and how of protein synthesis. *Nat. Rev. Mol. Cell Biol.*, **16**, 651–664.
23. Zoschke, R., Watkins, K.P. and Barkan, A. (2013) A rapid ribosome profiling method elucidates chloroplast ribosome behavior in vivo. *Plant Cell*, **25**, 2265–2275.
24. Rooijers, K., Loayza-Puch, F., Nijtmans, L.G. and Agami, R. (2013) Ribosome profiling reveals features of normal and disease-associated mitochondrial translation. *Nat. Commun.*, **4**, 2886.
25. Chotewutmontri, P. and Barkan, A. (2016) Dynamics of chloroplast translation during chloroplast differentiation in maize. *PLoS Genet.*, **12**, e1006106.
26. Haïli, N., Arnal, N., Quadrado, M., Amiar, S., Tcherkez, G., Dahan, J., Briozzo, P., Colas des Francs-Small, C., Vrielynck, N. and Mireau, H. (2013) The pentatricopeptide repeat MTSF1 protein stabilizes the nad4 mRNA in Arabidopsis mitochondria. *Nucleic Acids Res.*, **41**, 6650–6663.
27. Baudin-Baillieu, A., Hatin, I., Legendre, R. and Namy, O. (2016) Translation analysis at the genome scale by ribosome profiling. *Methods Mol. Biol.*, **1361**, 105–124.
28. Martin, M. (2015) Cutadapt removes adapter sequences from high-throughput sequencing reads. *EMBnet J.*, **17**, 10–12.
29. Langmead, B., Trapnell, C., Pop, M. and Salzberg, S.L. (2009) Ultrafast and memory-efficient alignment of short DNA sequences to the human genome. *Genome Biol.*, **10**, R25.
30. Li, H., Handsaker, B., Wysoker, A., Fennell, T., Ruan, J., Homer, N., Marth, G., Abecasis, G., Durbin, R. and 1000 Genome Project Data Processing Subgroup (2009) The Sequence Alignment/Map format and SAMtools. *Bioinformatics*, **25**, 2078–2079.
31. Köster, J. and Rahmann, S. (2012) Snakemake—a scalable bioinformatics workflow engine. *Bioinformatics*, **28**, 2520–2522.
32. Liao, Y., Smyth, G.K. and Shi, W. (2014) featureCounts: an efficient general purpose program for assigning sequence reads to genomic features. *Bioinformatics*, **30**, 923–930.
33. Love, M.I., Huber, W. and Anders, S. (2014) Moderated estimation of fold change and dispersion for RNA-seq data with DESeq2. *Genome Biol.*, **15**, 550.
34. Varet, H., Brillet-Guéguen, L., Coppée, J.-Y. and Dillies, M.-A. (2016) SARTools: a DESeq2- and edgeR-Based R pipeline for comprehensive differential analysis of RNA-Seq data. *PLoS One*, **11**, e0157022.
35. Huang, J., Struck, F., Matzinger, D.F. and Levings, C.S. (1994) Flower-enhanced expression of a nuclear-encoded mitochondrial respiratory protein is associated with changes in mitochondrion number. *Plant Cell*, **6**, 439–448.
36. Raczynska, K.D., Le Ret, M., Rurek, M., Bonnard, G., Augustyniak, H. and Gualberto, J.M. (2006) Plant mitochondrial genes can be expressed from mRNAs lacking stop codons. *FEBS Lett.*, **580**, 5641–5646.
37. Forner, J., Weber, B., Thuss, S., Wildum, S. and Binder, S. (2007) Mapping of mitochondrial mRNA termini in Arabidopsis thaliana: t-elements contribute to 5' and 3' end formation. *Nucleic Acids Res.*, **35**, 3676–3692.
38. Sultan, L.D., Milesina, D., Grewe, F., Rolle, K., Abudraham, S., Głodowicz, P., Niazi, A.K., Keren, I., Shevtsov, S., Klipcan, L. et al. (2016) The reverse transcriptase/RNA maturase protein MatR is required for the splicing of various group II introns in brassicaceae mitochondria. *Plant Cell*, **28**, 2805–2829.
39. Carrie, C., Wei enberger, S. and Soll, J.R. (2016) Plant mitochondria contain the protein translocase subunits TatB and TatC. *J. Cell Sci.*, **129**, 3935–3947.
40. Burger, G., Gray, M.W. and Lang, B.F. (2003) Mitochondrial genomes: anything goes. *Trends Genet.*, **19**, 709–716.
41. Amunts, A., Brown, A., Toots, J., Scheres, S.H.W. and Ramakrishnan, V. (2015) The structure of the human mitochondrial ribosome. *Science*, **348**, 95–98.
42. Greber, B.J., Bieri, P., Leibundgut, M., Leitner, A., Aebersold, R., Boehringer, D. and Ban, N. (2015) The complete structure of the 55S mammalian mitochondrial ribosome. *Science*, **348**, 303–308.
43. Desai, N., Brown, A., Amunts, A. and Ramakrishnan, V. (2017) The structure of the yeast mitochondrial ribosome. *Science*, **355**, 528–531.
44. Couvillion, M.T., Soto, I.C., Shipkovenska, G. and Churchman, L.S. (2016) Synchronized mitochondrial and cytosolic translation programs. *Nature*, **533**, 499–503.
45. Mai, N., Chrzanowska-Lightowlers, Z.M.A. and Lightowlers, R.N. (2017) The process of mammalian mitochondrial protein synthesis. *Cell Tissue Res.*, **367**, 5–20.
46. Salvato, F., Havelund, J.F., Chen, M., Rao, R.S.P., Rogowska-Wrzęsinska, A., Jensen, O.N., Gang, D.R., Thelen, J.J. and Møller, I.M. (2014) The potato tuber mitochondrial proteome. *Plant Physiol.*, **164**, 637–653.
47. Rao, R.S.P., Salvato, F., Thal, B., Eubel, H., Thelen, J.J. and Møller, I.M. (2017) The proteome of higher plant mitochondria. *Mitochondrion*, **33**, 22–37.
48. Li, G.-W., Burkhardt, D., Gross, C. and Weissman, J.S. (2014) Quantifying absolute protein synthesis rates reveals principles underlying allocation of cellular resources. *Cell*, **157**, 624–635.
49. Sonenberg, N. and Hinnebusch, A.G. (2009) Regulation of translation initiation in eukaryotes: mechanisms and biological targets. *Cell*, **136**, 731–745.
50. Shah, P., Ding, Y., Niemczyk, M., Kudla, G. and Plotkin, J.B. (2013) Rate-limiting steps in yeast protein translation. *Cell*, **153**, 1589–1601.
51. Kazama, T., Nakamura, T., Watanabe, M., Sugita, M. and Toriyama, K. (2008) Suppression mechanism of mitochondrial ORF79 accumulation by Rf1 protein in BT-type cytoplasmic male sterile rice. *Plant J.*, **55**, 619–628.
52. Uyttewaal, M., Arnal, N., Quadrado, M., Martin-Canadell, A., Vrielynck, N., Hiard, S., Gherbi, H., Bendahmane, A., Budar, F. and Mireau, H. (2008) Characterization of raphanus sativus pentatricopeptide repeat proteins encoded by the fertility restorer locus for ogura cytoplasmic male sterility. *Plant Cell*, **20**, 3331–3345.
53. Uyttewaal, M., Mireau, H., Rurek, M., Hammani, K., Arnal, N., Quadrado, M. and Giegé, P. (2008) PPR336 is associated with polysomes in plant mitochondria. *J. Mol. Biol.*, **375**, 626–636.
54. Li, G.-W., Oh, E. and Weissman, J.S. (2013) The anti-Shine–Dalgarno sequence drives translational pausing and codon choice in bacteria. *Nature*, **484**, 538–541.
55. O'Connor, P.B.F., Li, G.W., Weissman, J.S., Atkins, J.F. and Baranov, P.V. (2013) rRNA:mRNA pairing alters the length and the symmetry of mRNA-protected fragments in ribosome profiling experiments. *Bioinformatics*, **29**, 1488–1491.
56. Giegé, P., Hoffmann, M., Binder, S. and Brennicke, A. (2000) RNA degradation buffers asymmetries of transcription in Arabidopsis mitochondria. *EMBO Rep.*, **1**, 164–170.
57. Giegé, P., Sweetlove, L.J., Cognat, V. and Leaver, C.J. (2005) Coordination of nuclear and mitochondrial genome expression during mitochondrial biogenesis in Arabidopsis. *Plant Cell*, **17**, 1497–1512.
58. Holec, S., Lange, H., Kühn, K., Alioua, M., Börner, T. and Gagliardi, D. (2006) Relaxed transcription in Arabidopsis mitochondria is counterbalanced by RNA stability control mediated by polyadenylation and polynucleotide phosphorylase. *Mol. Cell Biol.*, **26**, 2869–2876.
59. Kühn, K., Obata, T., Feher, K., Bock, R., Fernie, A.R. and Meyer, E.H. (2015) Complete mitochondrial complex I deficiency induces an Up-Regulation of respiratory fluxes that is abolished by traces of functional complex I. *Plant Physiol.*, **168**, 1537–1549.
60. Kwasniak, M., Majewski, P., Skibior, R., Adamowicz, A., Czarna, M., Sliwinska, E. and Janska, H. (2013) Silencing of the nuclear RPS10 gene encoding mitochondrial ribosomal protein alters translation in Arabidopsis mitochondria. *Plant Cell*, **25**, 1855–1867.

Table S1 - Primers used for q-RT-PCR analysis

Gene / Exon	Forward Primer		Reverse Primer	
	Name	Sequence	Name	Sequence
<i>ccmFc</i> exon 2	CcmFC exon 2 F	AATCACTTCATGCCACCTC	CcmFC exon 2 R	GCGATTCTTCATCCACCAAT
<i>ccmFc</i> exon1	CcmFC exon 1 F	ATCTTTTTGCGGTGTGCTCT	CcmFC exon 1 R	ATTTCGTCTGTCTCATTCC
<i>cox2</i> exon 1	Cox2 exon1 F	GATTCTTCGGACCATCTTTCC	Cox2 exon1 R	TCCGATACCATTGATGTCCA
<i>cox2</i> exon2	Cox2 exon2 F	TCGTCTAGAAAGCTGTTCT	Cox2 exon2 R	TTGGGGGATTAATTGATTGG
<i>nad1</i> exon 1	Nad1a exon 1 F	TGATGTAGTGGGATCGTTCC	Nad1a exon 1 R	AGCCACTGGAGCCATTCTAA
<i>nad1</i> exon 2	Nad1b exon2 F	ATGCCTTTCTAGGAGCATTACG	Nad1b exon2 R	ACTTCATAAGAGACCATTTGAGCTG
<i>nad1</i> exon 3	Nad1b exon3 F	TGGTTTGGTATTCCTGTT	Nad1b exon3 R	TAATTCAGCTCCGCTTCTG
<i>nad1</i> exon 4	Nad1c exon4 F	TCTCAATGGGTCTGCTCT	Nad1c exon4 R	CATTAAGATCATATTGGCATACTCTCC
<i>nad1</i> exon 4	Nad1c exon5 F	TTAATGGGACTTGGCTGGAA	Nad1c exon5 R	AGGAAGCCATTGAAAGGTGA
<i>nad2</i> exon 1	Nad2a exon1 F	TTTAGCGGTTTTCCAGAGA	Nad2a exon1 R	TAATCAAAGCCAAACCACAT
<i>nad2</i> exon 2	Nad2a exon2 F	GGCTGGTACCATTTCTGATGT	Nad2a exon2 R	TGAGCCGAGATCATAAAGAGC
<i>nad2</i> exon 3	Nad2b exon3 F	CTGGAGCTACCACTTCGAT	Nad2b exon3 R	CGAAAAGGAACTGCAGTGAT
<i>nad2</i> exon 4	Nad2b exon4 F	GGATGCATTCGCCATAGTTT	Nad2b exon4 R	GGGGTATTCTCGTATGAG
<i>nad2</i> exon 5	Nad2b exon5 F	TTTTTGATACACCTAGGACATGGAT	Nad2b exon5 R	ATGAACTGAGTGCATTTGATG
<i>nad4</i> exon1	Nad4 exon1 F	TTGCATTTTGTGGGTTGGTC	Nad4 exon1 R	TAGGGATTAGCACGCTTTTCG
<i>nad4</i> exon2	Nad4 exon2 F	GGAGTATGGGTTTCGAGACA	Nad4 exon2 R	AAATCGTGTGTTCTGTTTG
<i>nad4</i> exon3	Nad4 exon3 F	CCATGCCGAATTTTTCTACC	Nad4 exon3 R	GCGCTGTAATGTGGCTACT
<i>nad4</i> exon 4	Nad4 exon4 F	GATGGGTGTTACCCAAAG	Nad4 exon4 R	TGAAATTTGCCATGTTGCAC
<i>nad5</i> exon 1	Nad5a exon1 F	GCTCGGTAGTCCGTAGCAG	Nad5a exon1 R	AGCGCGACTTCATAAAAGC
<i>nad5</i> exon 2	Nad5a exon2 F	ATTGGTCTGTGGGAAATC	Nad5a exon2 R	AAAGGGGAGCACCTTGCTAT
<i>nad5</i> exon 4	Nad5c exon4 F	GCCTTTGCAATGTACTTGG	Nad5c exon4 R	TCAAAATGAAAGCAGCATGATTA
<i>nad7</i> exon1	Nad7 exon1 F	GACCTCAACATCCTGCTGCT	Nad7 exon1 R	CCACCATTCTCCGTTCACT
<i>nad7</i> exon2	Nad7 exon2 F	GAGGGACTGAGAAATTAAGAGTACA	Nad7 exon2 R	GATCAAAATAAGTAAAGCTGAAGA
<i>nad7</i> exon3	Nad7 exon3 F	GCTATGGATGTGGGAGCATT	Nad7 exon3 R	AGGCAGATCTTGCCACTC
<i>nad7</i> exon4	Nad7 exon4 F	GTATGCTGGGATTTCGGAAG	Nad7 exon4 R	CATTGCACAATGATCCGAAG
<i>nad7</i> exon5	Nad7 exon5 F	ATACCCGAGTTGAAGCACCT	Nad7 exon5 R	TCCTTGTAATGGGCAAAGC
<i>rpl2</i> exon1	Rpl2 exon1 F	TGATGGCCGTTATGTAGTG	Rpl2 exon1 R	TTTGAGAGGAGAAGGCAGA
<i>rpl2</i> exon2	Rpl2 exon2 F	GAAGCAGGCAAATGGTGAT	Rpl2 exon2 R	ACACAGTGAATAAGGGCTTAGGA
<i>rps3</i> exon1	Rps3 exon1 F	CCGATTTCCGGTAAGACTTGG	Rps3 exon1 R	CACTGAACCGACTTGAATCTGA
<i>rps3</i> exon2	Rps3 exon2 F	AGGTTGACCCACTTCATTG	Rps3 exon2 R	GTTCCCGAGCATCAAGGTTA
<i>nad9</i>	QM0070F	GGATGACCTCGAAACCATA	QM0070R	CACGATTCGTGTACAAACC
<i>rpl16</i>	QM0080F	GAGCATTTGCCAAACTCACA	QM0080R	CGGACACTTTCATCGTGCTA
<i>ccmB</i>	QM0110F	TCTTGGAAATCACATCCAGCA	QM0110R	CGAGACCGAAATTGGAAAAA
<i>rpl5</i>	QM0210F	AAGGGGTTTCGACAGGAAAGT	QM0210R	CGTATTTTCGACCGGAAATC
<i>cob</i>	QM0220F	TGCCGGAATGGTATTTCTA	QM0220R	GCCAAAAGCAACCAAAACAT
<i>nad6</i>	QM0270F	TCGTCTGGAATACATCCTGTCT	QM0270R	GTGAGTGGGTGAGTCTGCTCT
<i>rps4</i>	QM0290F	ACCCATCACAGAGATGCACA	QM0290R	TCACACAAACCTTCGATGA
<i>atp6-1</i>	QM0410F	TCTTTTTCGAGTCAATGCAC	QM0410R	TCTCGGTATCTCATTGTC
<i>atp8</i>	QM0480F	CCGTGACTTATTGGGAAAA	QM0480R	TTCCTTGGCCATGTACAACA
<i>matR</i>	QM0520F	AATTTTTCGAGAGCTGGAA	QM0520R	TTGAACCCGCTCTGTAGAC
<i>mttb</i>	QM0570F	GGGGTCTTTCTTTGAAACC	QM0570R	TCTCCCTCATTCCACTCGTC
<i>atp4</i>	QM0640F	GGATCAGCTTGCGAATTTGT	QM0640R	GCAAATTCCTCCCACTAA
<i>nad4L</i>	QM0650F	GGGGAATCCTCCTTAATAGACG	QM0650R	AACGAAAATGGCTAACCCAATA
<i>cox3</i>	QM0730F	CCGTAACCTGGGCTCATCAT	QM0730R	AAACCATGAAAGCCTGTTGC
<i>ccmFN1</i>	QM0830F	AGCTCTTGGCATTGCTTTGT	QM0830R	AGTGCCACAATCCATTTCAT
<i>ccmC</i>	QM0900F	AGCTACGCGCAAATTCAT	QM0900R	GCCGTGGCGATATAAACAAT
<i>ccmFN2</i>	QM0960F	CGTGTCTTCGTAATGGAAA	QM0960R	TGATAAGCCCACTTCC
<i>rps12</i>	QM0980F	AGCCAAAGTACGGTTGAGCA	QM0980R	TTTGGGTTTTCTGCACCAT
<i>nad3</i>	QM0990F	CGAATGTGGTTTCGATCCTT	QM0990R	GACCCCTTTTCCATTCTA
<i>atp9</i>	QM1080F	GGAGCTGCTATCGGTATTGG	QM1080R	TAGAGCAAAGCCCAAAATGG
<i>atp6-2</i>	QM1170F	GCTTGGCAATCCTTGGTAGA	QM1170R	GACCAAGATGCAAGGAAAA
<i>atp1</i>	QM1190F	TCACTTCGACACGTCTTTGC	QM1190R	GGAATGGCCTTGAACTTGA
<i>rps7</i>	QM1270F	CTCGAAGTGAACGCGATGTA	QM1270R	AAGCTGCTCAAGGATCCAA
<i>cox1</i>	QM1360F	GTAGTGCAGTGAAGTAGGC	QM1360R	CTGCTGGATTGCGTATCAT
rRNA 26S (mt)	QMR26SF	GACGAGACTTTCCCTTTTG	QMR26SR	CTTGGAGCGAATGGATGAT
rRNA 18S (nuc)	nuc18S_F	AAACGGCTACCACATCCAAG	nuc18S_R	ACTCGAAAGAGCCGGTATT

Table S2: C-to-U transition efficiencies of mitochondrial editing sites calculated from total (RNASEQ) and ribosome-associated (RIBOSEQ) RNA samples.

Each site are identified by the transcript to which they belong and its position relatively to the first base of the translational start codon (TrPos). Numbers of reads identified per sites (Coverage) are also indicated.

NA: Not applicable

GeneName	TrPos	Observed_RNASEQ	Observed_RIBOSEQ	Coverage_RNASEQ	Coverage_RIBOSEQ
atp1	1470	0,14	0,09	8625	2268
atp1	1538	0,99	1	6755	4321
atp1	1652	0,99	1	5143	3467
atp1	1775	0,99	1	2544	680
atp1	1844	0,99	1	4428	2658
atp4	409	0,05	0,1	768	105
atp4	647	0,16	0,24	1324	41
atp4	515	0,82	0,83	2388	1636
atp4	403	0,93	0,99	714	100
atp4	681	0,98	1	849	427
atp4	354	0,99	1	1119	59
atp4	480	0,99	1	1934	49
atp4	660	0,99	1	1136	31
atp4	513	1	1	2166	1263
atp4	516	1	1	2397	1687
atp9	136	0,99	1	28353	3302
atp9	166	0,99	1	15368	520
atp9	250	0,99	1	17847	1770
atp9	307	1	1	26108	370
ccmB	639	0	NA	95	3
ccmB	640	0,02	NA	95	3
ccmB	580	0,03	0	197	46
ccmB	277	0,06	0,17	109	12
ccmB	715	0,08	NA	79	7
ccmB	545	0,22	0,3	251	23
ccmB	651	0,27	0,96	120	28
ccmB	653	0,33	1	125	28
ccmB	735	0,55	1	77	13
ccmB	690	0,61	NA	141	2
ccmB	693	0,62	NA	134	2
ccmB	425	0,71	NA	268	5
ccmB	443	0,75	0,94	301	16
ccmB	477	0,77	1	338	55
ccmB	167	0,82	NA	240	9
ccmB	506	0,89	1	262	18
ccmB	518	0,93	NA	304	6
ccmB	267	0,95	NA	130	2
ccmB	563	0,99	1	254	53
ccmB	519	0,99	NA	305	5
ccmB	606	0,99	NA	162	5
ccmB	276	1	1	132	11
ccmB	567	1	1	234	53
ccmB	210	1	NA	163	7
ccmB	614	1	NA	126	5
ccmB	615	1	NA	123	5
ccmC	1059	0,05	0	227	14
ccmC	864	0,07	0,09	255	35
ccmC	735	0,17	0,25	155	16
ccmC	814	0,93	NA	122	0
ccmC	667	0,94	0,99	244	199

ccmC	1139	0,94	NA	18	4
ccmC	883	0,95	1	293	18
ccmC	586	0,95	NA	204	4
ccmC	662	0,96	1	244	206
ccmC	980	0,96	1	323	18
ccmC	616	0,96	NA	228	4
ccmC	1004	0,97	1	380	28
ccmC	1031	0,97	NA	361	3
ccmC	878	0,98	1	277	19
ccmC	950	0,99	0,96	369	82
ccmC	929	0,99	1	372	36
ccmC	941	0,99	1	357	15
ccmC	1051	0,99	NA	320	1
ccmC	1091	0,99	NA	121	7
ccmC	904	1	1	240	45
ccmC	919	1	1	364	40
ccmC	1058	1	1	245	14
ccmC	1133	1	NA	18	3
ccmC	1156	NA	NA	6	5
ccmFC	1048	0,01	0	563	31
ccmFC	1273	0,02	0	523	14
ccmFC	684	0,1	0,26	603	62
ccmFC	501	0,14	0,33	619	68
ccmFC	1338	0,25	0,48	371	21
ccmFC	456	0,38	0,22	405	41
ccmFC	173	0,53	1	333	20
ccmFC	298	0,54	0,74	203	23
ccmFC	529	0,64	0,78	819	18
ccmFC	457	0,64	0,98	404	41
ccmFC	538	0,66	0,88	842	40
ccmFC	226	0,71	1	297	17
ccmFC	1403	0,74	0,76	588	38
ccmFC	1369	0,76	1	339	23
ccmFC	246	0,77	NA	212	0
ccmFC	1450	0,89	1	560	22
ccmFC	283	0,9	NA	126	2
ccmFC	1295	0,91	0,96	427	27
ccmFC	245	0,95	NA	209	0
ccmFC	278	0,99	NA	153	0
ccmFC	269	1	NA	180	0
ccmFN1	348	0	NA	153	3
ccmFN1	632	0,01	0,07	143	118
ccmFN1	519	0,15	0,06	53	18
ccmFN1	526	0,78	1	37	26
ccmFN1	857	0,79	NA	180	1
ccmFN1	437	0,93	0,93	120	56
ccmFN1	305	0,93	NA	85	6
ccmFN1	1103	0,96	0,97	273	72
ccmFN1	858	0,96	NA	180	1
ccmFN1	291	0,97	1	120	23
ccmFN1	939	0,97	NA	284	3
ccmFN1	417	0,98	1	129	14
ccmFN1	252	0,98	NA	197	4
ccmFN1	410	0,99	1	131	21
ccmFN1	927	0,99	1	255	28
ccmFN1	954	0,99	NA	310	6
ccmFN2	821	0,15	0,11	211	46

ccmFN2	936	0,79	NA	102	3
ccmFN2	904	0,8	NA	70	10
ccmFN2	1005	0,85	NA	190	1
ccmFN2	1048	0,87	0,9	133	21
ccmFN2	954	0,89	1	187	123
ccmFN2	793	0,9	0,95	263	19
ccmFN2	1119	0,91	0,98	189	41
ccmFN2	1072	0,92	1	102	45
ccmFN2	1084	0,93	1	95	49
ccmFN2	987	0,93	NA	217	1
cob	2512	0,13	0,07	816	897
cob	2826	0,17	0,11	1743	93
cob	2227	0,97	1	1140	100
cob	2020	0,98	1	1541	105
cob	2470	0,99	1	885	97
cob	2755	0,99	1	1692	631
cob	2810	0,99	1	1583	86
cob	2884	0,99	1	1656	210
cob	2188	0,99	NA	2054	8
cob	2986	1	1	2777	119
cox2	229	0,72	0,75	2630	55
cox2	342	0,78	0,93	2280	101
cox2	231	0,92	1	2467	202
cox2	482	0,97	0,99	3184	216
cox2	275	0,97	1	3088	2175
cox2	457	0,98	1	3738	1812
cox2	785	0,98	1	2986	1643
cox2	925	0,99	0,99	1340	1168
cox2	583	0,99	1	3570	10647
cox2	680	0,99	1	2983	4508
cox2	761	0,99	1	3046	14751
cox2	946	1	0,99	252	178
cox2	902	1	1	3188	2250
cox3	980	0,05	0,19	3422	21
cox3	1224	0,51	0,51	4025	158
cox3	1257	0,83	0,8	2667	15
cox3	1361	0,85	1	527	70
cox3	1305	0,93	1	800	20
cox3	634	0,97	0,99	2910	400
cox3	799	0,98	0,99	1706	272
cox3	489	0,98	1	1714	109
cox3	688	0,98	1	1180	819
cox3	691	0,98	1	1330	798
cox3	790	0,98	1	1962	129
cox3	622	0,99	1	3366	381
matR	1625	0,53	NA	246	1
matR	1622	0,61	NA	263	1
matR	1760	0,81	NA	535	1
matR	403	0,9	1	315	13
matR	1836	0,92	0,55	373	11
matR	490	0,94	NA	444	6
matR	1780	0,94	NA	616	0
matR	1800	0,94	NA	510	0
matR	1924	0,96	NA	290	1
matR	1759	0,97	NA	540	1
mttb	696	0,17	0,23	418	43
mttb	730	0,19	0,2	386	15

mttb	531	0,37	NA	371	7
mttb	288	0,46	0,36	407	36
mttb	618	0,52	NA	582	9
mttb	810	0,53	0,59	351	37
mttb	725	0,72	0,73	397	26
mttb	849	0,82	0,74	554	35
mttb	890	0,82	0,75	274	16
mttb	241	0,87	0,97	728	34
mttb	584	0,88	0,94	396	18
mttb	203	0,9	1	323	15
mttb	649	0,94	0,97	449	38
mttb	837	0,96	0,98	471	51
mttb	289	0,96	1	384	39
mttb	505	0,96	NA	390	2
mttb	508	0,96	NA	395	2
mttb	787	0,96	NA	405	8
mttb	793	0,96	NA	396	4
mttb	674	0,97	1	394	18
mttb	682	0,99	1	410	49
mttb	809	0,99	1	352	37
mttb	844	0,99	1	540	46
mttb	731	1	NA	386	9
nad1	1467	0,91	0,96	1259	52
nad1	1399	0,92	1	2457	443
nad1	951	0,94	1	661	604
nad1	952	0,94	1	660	622
nad1	1180	0,95	0,99	923	372
nad1	1542	0,96	0,99	1628	377
nad1	909	0,96	1	510	857
nad1	1215	0,96	1	910	34
nad1	1387	0,96	1	2507	706
nad1	1224	0,98	0,99	939	2055
nad1	1279	0,98	0,99	1018	378
nad1	1318	0,98	0,99	1055	177
nad1	811	0,98	1	529	48
nad1	1136	0,99	0,99	495	215
nad1	1020	0,99	1	535	557
nad1	1369	0,99	1	1367	172
nad1	1137	1	0,99	530	255
nad1	1134	1	1	486	168
nad2	406	0,04	0,01	797	182
nad2	763	0,09	0,05	1154	777
nad2	1357	0,15	0,08	1066	336
nad2	679	0,28	0,25	654	296
nad2	149	0,66	0,67	919	42
nad2	211	0,87	NA	575	7
nad2	1560	0,91	NA	321	10
nad2	1403	0,94	0,95	632	181
nad2	465	0,95	0,98	1177	60
nad2	462	0,95	1	1142	51
nad2	1557	0,95	NA	357	8
nad2	180	0,97	1	639	25
nad2	548	0,97	1	876	113
nad2	582	0,97	1	712	28
nad2	945	0,97	1	781	20
nad2	1404	0,98	0,98	619	173
nad2	510	0,98	1	977	146

nad2	816	0,98	1	909	1160
nad2	966	0,98	1	604	32
nad2	1215	0,98	1	858	29
nad2	210	0,98	NA	574	8
nad2	1284	0,98	NA	637	10
nad2	1077	0,99	0,99	934	157
nad2	515	0,99	1	1004	164
nad2	521	0,99	1	1013	867
nad2	651	0,99	1	750	621
nad2	1085	0,99	1	940	229
nad2	1115	0,99	1	871	317
nad2	1119	0,99	1	942	212
nad2	1433	1	0,99	737	84
nad2	1614	NA	1	10	88
nad3	377	0,84	0,99	403	143
nad3	580	0,84	0,99	415	193
nad3	292	0,85	0,99	195	451
nad3	236	0,87	1	582	109
nad3	575	0,88	1	404	240
nad3	254	0,89	1	638	179
nad3	482	0,89	1	344	2441
nad3	311	0,9	0,99	213	235
nad3	478	0,91	1	329	2615
nad3	439	0,94	1	273	506
nad3	440	0,94	1	274	521
nad4	645	0,02	0	1133	204
nad4	974	0,05	0,07	691	232
nad4	1628	0,11	0,21	1372	233
nad4	1358	0,13	0	1786	23
nad4	1433	0,19	0,1	1772	254
nad4	311	0,27	0,27	1390	812
nad4	1328	0,83	0,75	1739	208
nad4	1063	0,96	0,97	1562	319
nad4	391	0,97	0,96	971	229
nad4	256	0,98	0,99	1245	80
nad4	1644	0,98	0,99	1454	1175
nad4	886	0,98	1	1701	433
nad4	1660	0,98	1	848	2708
nad4	630	0,99	0,99	1134	587
nad4	351	0,99	1	1394	197
nad4	393	0,99	1	962	270
nad4	544	0,99	1	1076	357
nad4	589	0,99	1	1046	11
nad4	603	0,99	1	1170	153
nad4	835	0,99	1	974	151
nad4	1011	0,99	1	860	16
nad4	1123	0,99	1	1293	396
nad4	1204	0,99	1	1868	597
nad4	1237	0,99	1	2665	335
nad4	1375	0,99	1	1664	11
nad4	1399	0,99	1	1364	190
nad4	1582	0,99	1	2142	40
nad4	1600	0,99	1	1567	125
nad4	1632	0,99	1	1528	243
nad4	301	0,99	NA	1377	4
nad4	334	1	1	1116	1811
nad4	385	1	1	1166	158

nad4	424	1	1	612	252
nad4	663	1	1	1079	258
nad4	664	1	1	1067	258
nad4	676	1	1	975	91
nad4	1260	1	1	2811	169
nad4	1356	1	1	1786	23
nad4L	358	0,97	0,99	811	150
nad4L	514	0,97	1	2641	370
nad4L	417	0,98	0,97	1810	37
nad4L	448	0,98	0,97	2630	718
nad4L	505	0,98	0,99	2475	159
nad4L	372	0,99	0,98	754	178
nad4L	427	0,99	1	1765	299
nad4L	475	0,99	1	2839	648
nad4L	403	1	1	1576	11
nad4L	412	1	1	1691	18
nad5	2000	0,04	0	609	5513
nad5	1802	0,06	0,05	4455	1270
nad5	1736	0,09	0,05	2710	504
nad5	872	0,21	0,21	1642	76
nad5	680	0,71	0,82	802	124
nad5	343	0,93	1	730	227
nad5	445	0,95	1	834	406
nad5	1681	0,95	1	1258	291
nad5	226	0,96	1	945	1079
nad5	1621	0,96	1	1993	47
nad5	679	0,97	1	802	124
nad5	906	0,97	1	1529	570
nad5	946	0,97	1	1392	129
nad5	2029	0,97	1	312	248
nad5	313	0,98	0,98	743	776
nad5	469	0,98	1	672	328
nad5	624	0,98	1	1100	305
nad5	747	0,98	1	1059	224
nad5	784	0,98	1	1736	1607
nad5	796	0,98	1	2183	1349
nad5	835	0,98	1	2291	80
nad5	1651	0,98	1	1242	84
nad5	1966	0,98	1	508	87
nad5	1989	0,98	1	576	281
nad5	565	0,98	NA	1208	6
nad5	429	0,99	1	1139	22
nad5	619	0,99	1	1129	440
nad5	700	0,99	1	1334	92
nad5	934	0,99	1	1153	390
nad5	1561	0,99	1	1140	221
nad5	669	1	1	1003	189
nad5	1346	1	1	1468	110
nad5	1987	1	1	586	220
nad6	106	0,84	NA	3069	6
nad6	231	0,97	1	1611	96
nad6	273	0,99	0,97	1167	67
nad6	267	0,99	0,98	1342	49
nad6	204	0,99	1	2641	151
nad6	624	0,99	1	1752	64
nad6	641	0,99	1	1500	72
nad6	266	1	1	1346	49

nad6	339	1	1	1385	151
nad6	347	1	1	1131	147
nad6	369	1	NA	443	3
nad7	1163	0,06	0,12	1116	371
nad7	1424	0,13	0,1	2321	494
nad7	336	0,31	0,51	1112	1845
nad7	1511	0,49	0,3	1337	30
nad7	1169	0,52	0,69	1200	252
nad7	412	0,88	0,98	716	767
nad7	398	0,91	1	829	468
nad7	1337	0,93	1	1789	125
nad7	1072	0,96	0,98	1481	52
nad7	1300	0,97	0,97	1287	117
nad7	451	0,97	1	501	60
nad7	718	0,97	1	848	19
nad7	625	0,98	0,99	718	142
nad7	690	0,98	1	581	159
nad7	709	0,98	1	950	118
nad7	1431	0,98	1	1909	406
nad7	1462	0,98	1	2424	359
nad7	1498	0,98	1	1397	43
nad7	1053	0,99	0,79	1136	71
nad7	587	0,99	0,97	453	144
nad7	511	0,99	1	789	541
nad7	574	0,99	1	708	240
nad7	583	0,99	1	547	240
nad7	618	0,99	1	693	179
nad7	1098	0,99	1	1375	341
nad7	1113	0,99	1	1533	645
nad7	1143	0,99	1	1095	825
nad7	1453	0,99	1	2849	366
nad7	1477	0,99	1	2642	45
nad7	952	1	1	2200	703
nad7	1108	1	1	1365	718
nad9	499	0,97	1	2547	290
nad9	599	0,98	1	2411	223
nad9	293	0,99	1	1995	690
nad9	368	0,99	1	1812	202
nad9	391	0,99	1	1632	169
nad9	529	0,99	1	2074	297
nad9	640	0,99	1	3142	2182
rpl16	505	0,94	NA	1115	10
rpl16	208	0,95	0,86	1713	21
rpl16	439	0,97	1	1783	17
rpl16	511	0,97	1	943	19
rpl16	33	NA	NA	0	0
rpl16	60	NA	NA	0	0
rpl2	489	0,03	0,05	794	19
rpl2	908	0,07	0,1	1142	69
rpl2	409	0,75	0,75	691	12
rpl5	579	0,01	0,07	446	68
rpl5	516	0,7	0,78	522	117
rpl5	493	0,91	1	705	52
rpl5	550	0,91	1	454	119
rpl5	627	0,93	0,99	458	165
rpl5	970	0,93	0,99	468	124
rpl5	775	0,95	0,99	534	74

rpl5	505	0,96	0,99	564	135
rpl5	787	0,97	1	415	33
rps12	329	0,74	0,98	218	54
rps12	128	0,87	0,98	710	107
rps12	265	0,9	1	310	14
rps12	148	0,91	1	519	62
rps12	328	0,93	1	219	60
rps12	313	0,94	1	320	100
rps12	240	0,96	1	391	20
rps12	190	0,98	NA	531	9
rps3	677	0,02	0	693	37
rps3	288	0,02	0,02	1196	198
rps3	349	0,04	0	957	13
rps3	1742	0,04	NA	72	0
rps3	1422	0,07	NA	683	4
rps3	1506	0,37	0,52	520	33
rps3	765	0,55	0,47	816	15
rps3	1696	0,75	NA	737	3
rps3	1049	0,77	0,88	929	32
rps3	1632	0,83	0,91	674	11
rps3	1733	0,83	NA	288	0
rps3	1514	0,89	0,97	512	35
rps3	226	0,93	0,98	772	41
rps4	255	0,86	NA	304	6
rps4	1072	0,87	0,97	329	34
rps4	204	0,87	NA	369	4
rps4	1071	0,88	0,94	336	36
rps4	406	0,88	1	184	66
rps4	117	0,9	0,99	459	485
rps4	264	0,9	NA	274	1
rps4	996	0,91	1	685	11
rps4	361	0,92	0,97	154	36
rps4	328	0,93	NA	365	8
rps4	985	0,94	0,95	747	20
rps4	337	0,94	NA	290	4
rps4	1021	0,95	0,98	557	94
rps4	553	0,95	NA	325	7
rps4	106	0,96	0,98	637	108
rps7	242	0,01	NA	199	8
rps7	231	0,11	NA	309	6
rps7	779	0,87	0,96	140	57

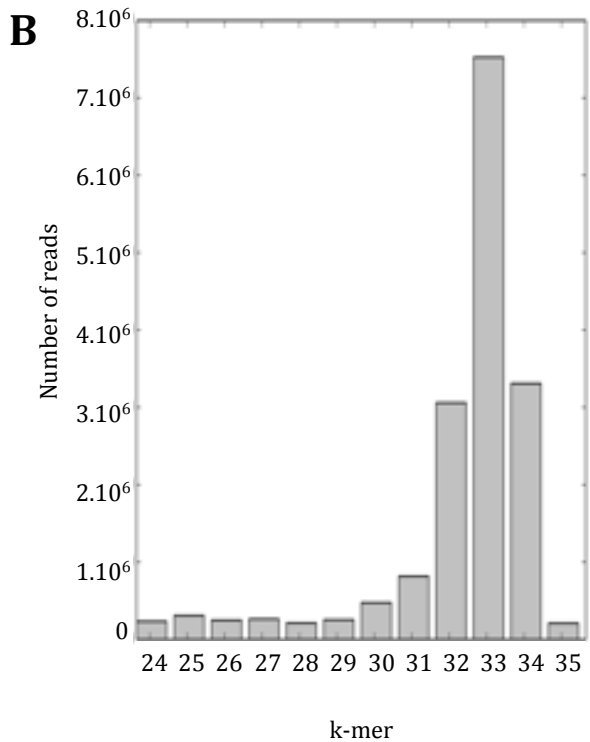
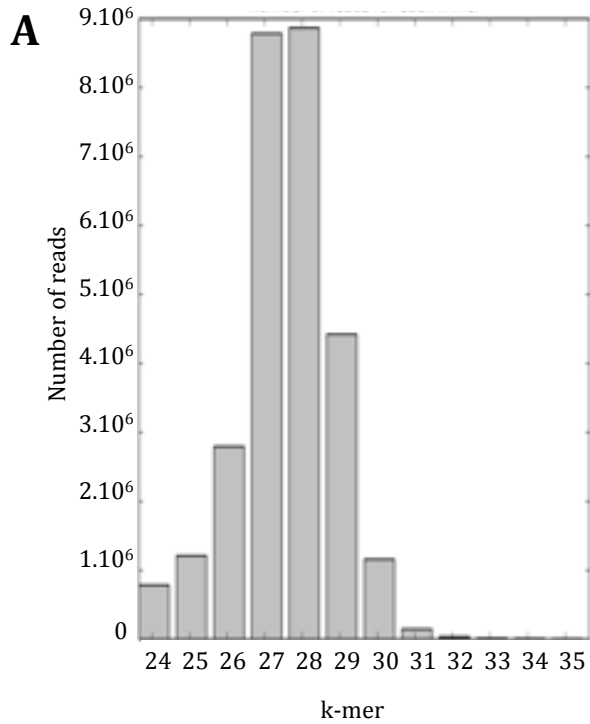


Figure S1: K-mer distributions in the 27 and 33-mers short RNA populations. A. Quantification of sequencing results indicates that the 27-mers population is predominantly composed of 27, 28 and 29-base fragments. B. As shown, the 33-mer RNAs are predominantly composed of 32, 33 and 34-nucleotide fragments.

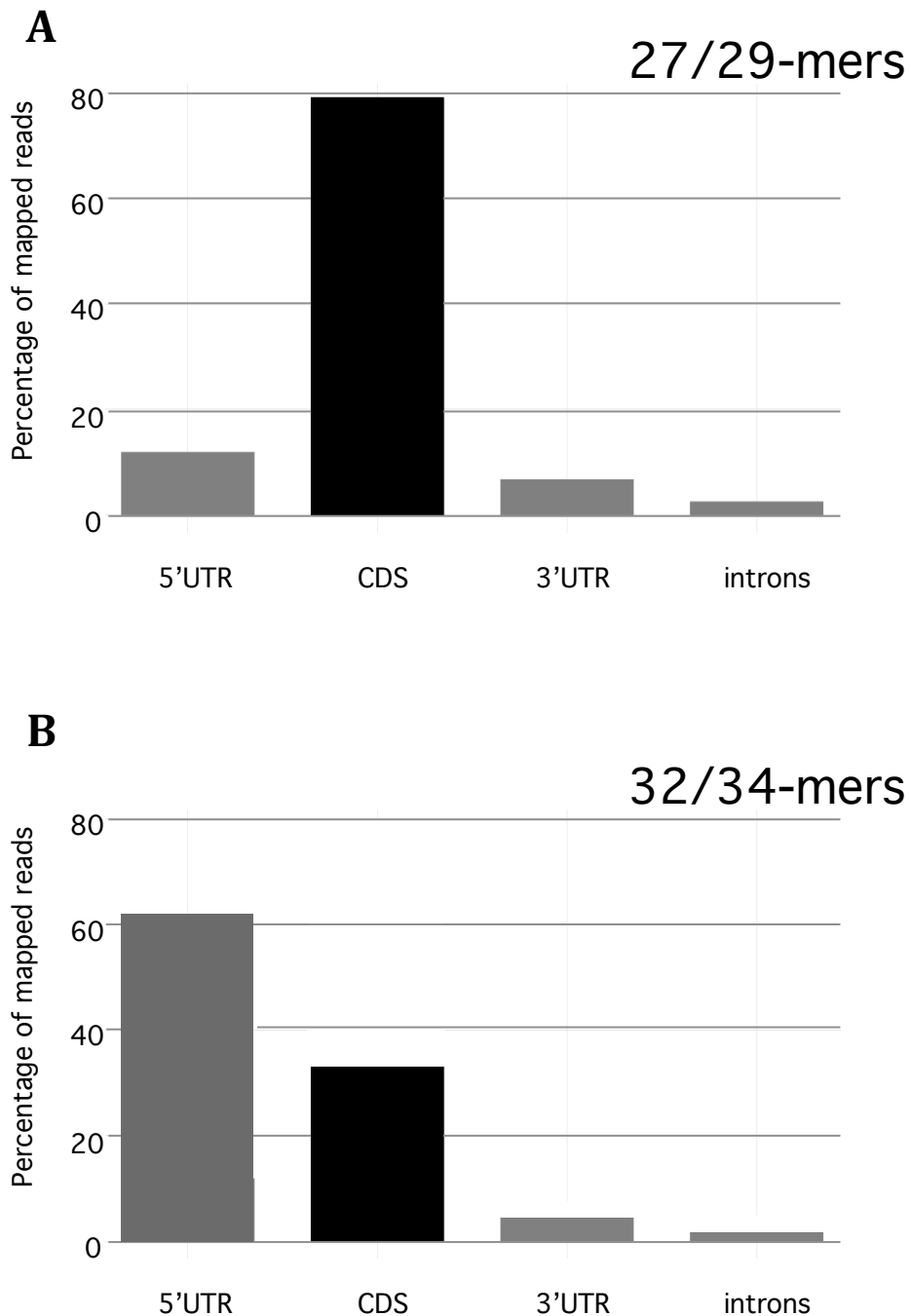


Figure S2: Most reads derived from the 27-mer population map to the mitochondrial coding sequences.

A. Reads derived from the 27-mer population were aligned against the Arabidopsis mitochondrial genes (from the Col-0 accession). As shown, 12 % of them aligned to 5'UTRs, 79 % to CDS, 7 % to 3'UTR and 2 % to introns.

B. In contrast, only 33% of the 32/34-mers align with mitochondrial CDS, as most of them (62%) of them align to genes' 5' UTRs.

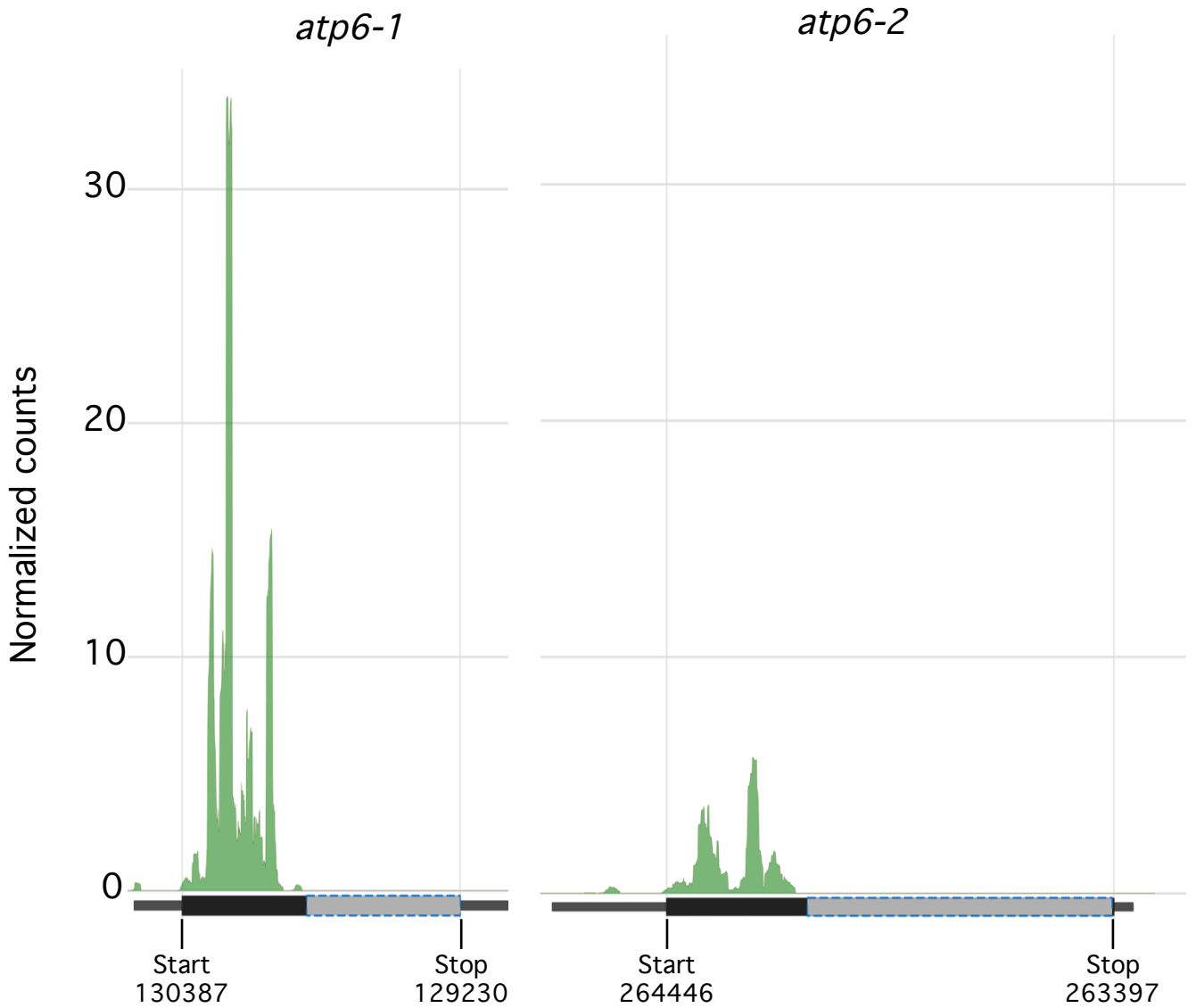


Figure S3: Comparative RPF densities along the *atp6-1* and *atp6-2* transcripts. Only RPF densities aligning in the 5' coding regions distinguishing the two copies of *atp6* are shown. The coordinates of start and stop codons of both genes in the Col-0 mitochondrial genome are indicated.

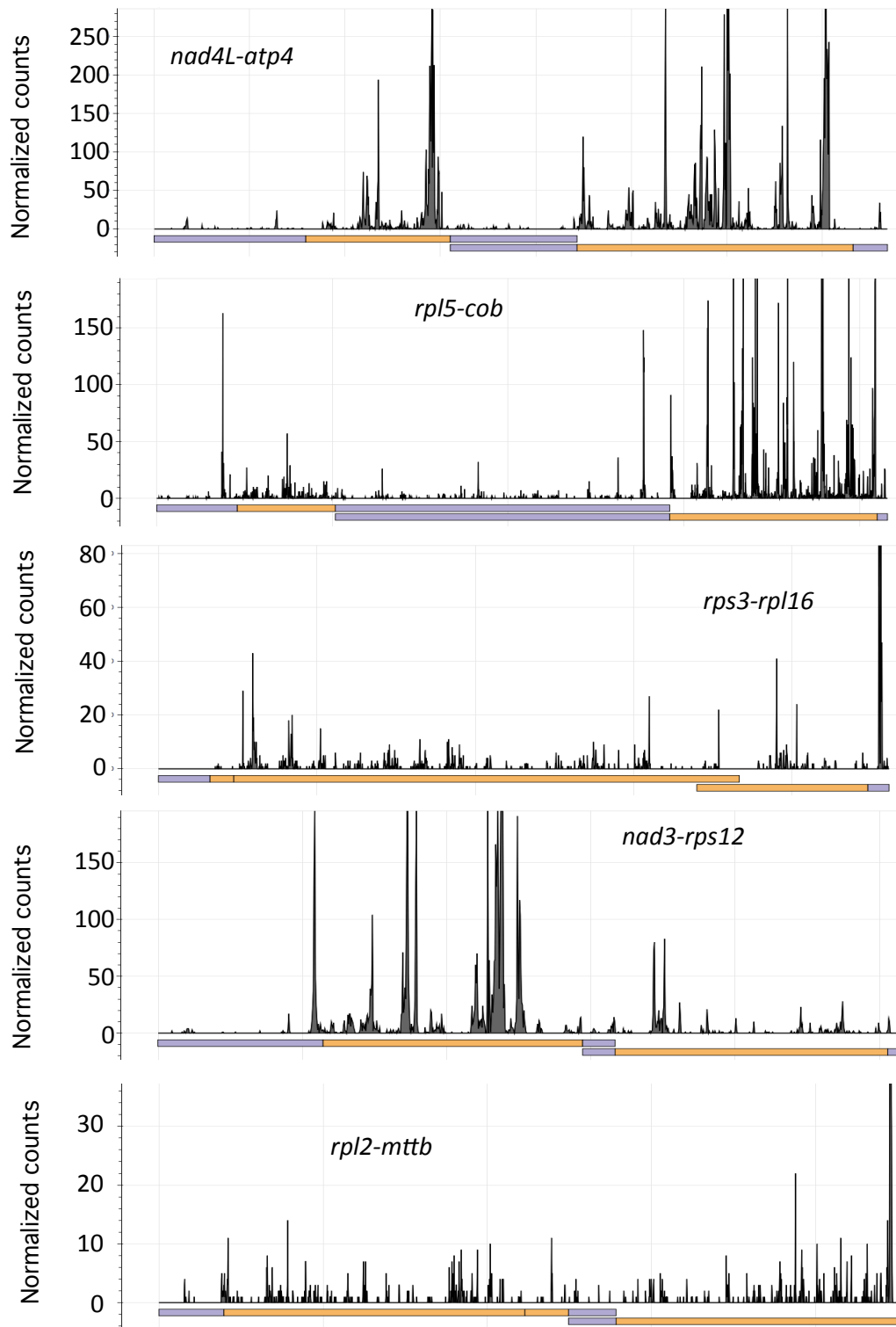


Figure S4: RPF coverage along the di-cistronic mRNAs encoded in Arabidopsis mitochondria.

RPF densities, normalized by both mRNA length and abundance, are shown. Coding sequences and UTRs are delimited with yellow and blues lines respectively.

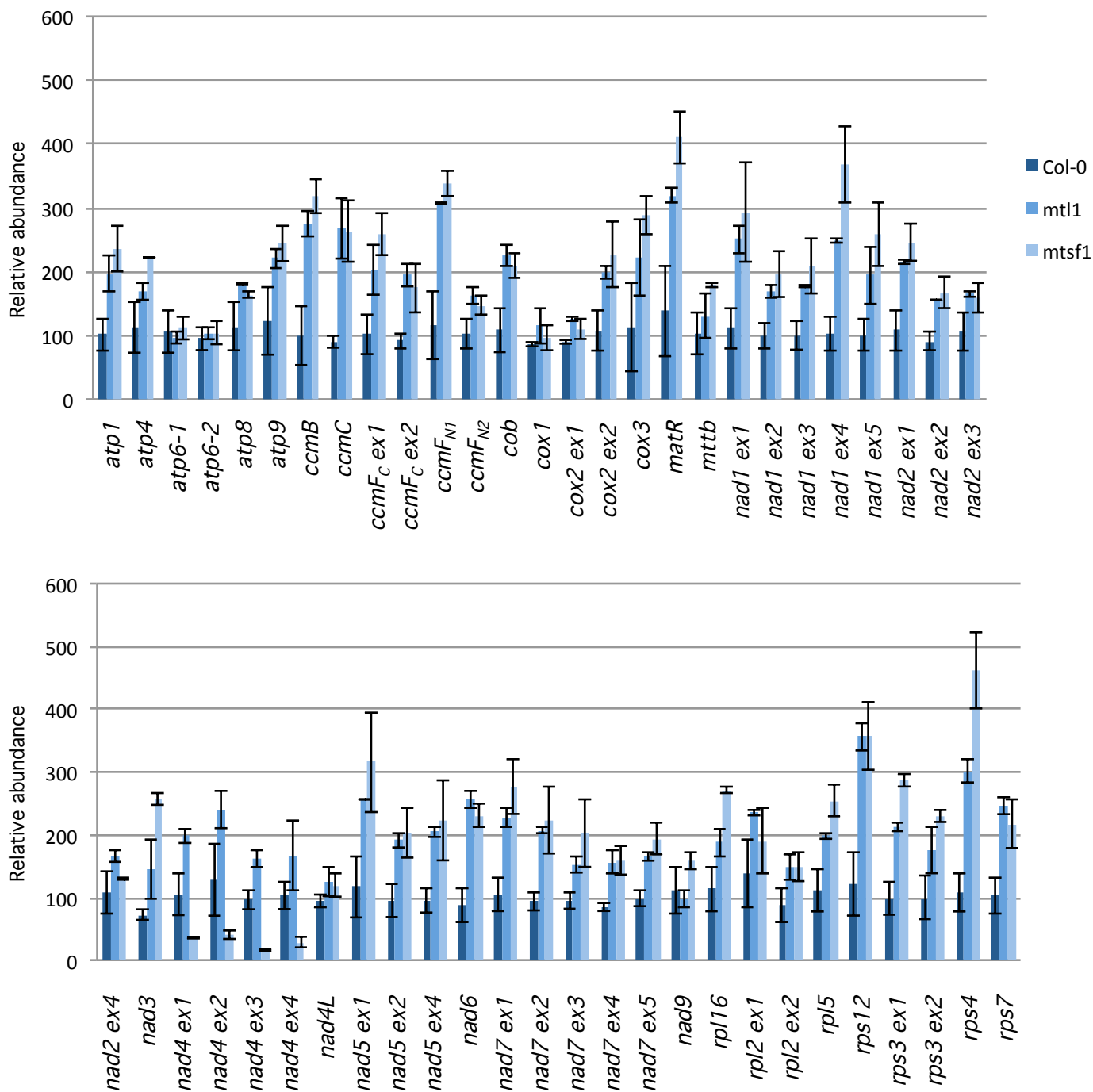


Figure S5: Quantitative RT-PCR analysis measuring the steady state levels of mitochondrial mRNAs exon by exon in the indicated genotypes (Col-0, *mtl1*, *mts1*). Numbers represent relative abundances to nuclear 18s rRNA. Values of each exon obtained in the wild type were arbitrarily set to 100; values obtained in the mutants are indicated accordingly. Means \pm SE (n = 3).

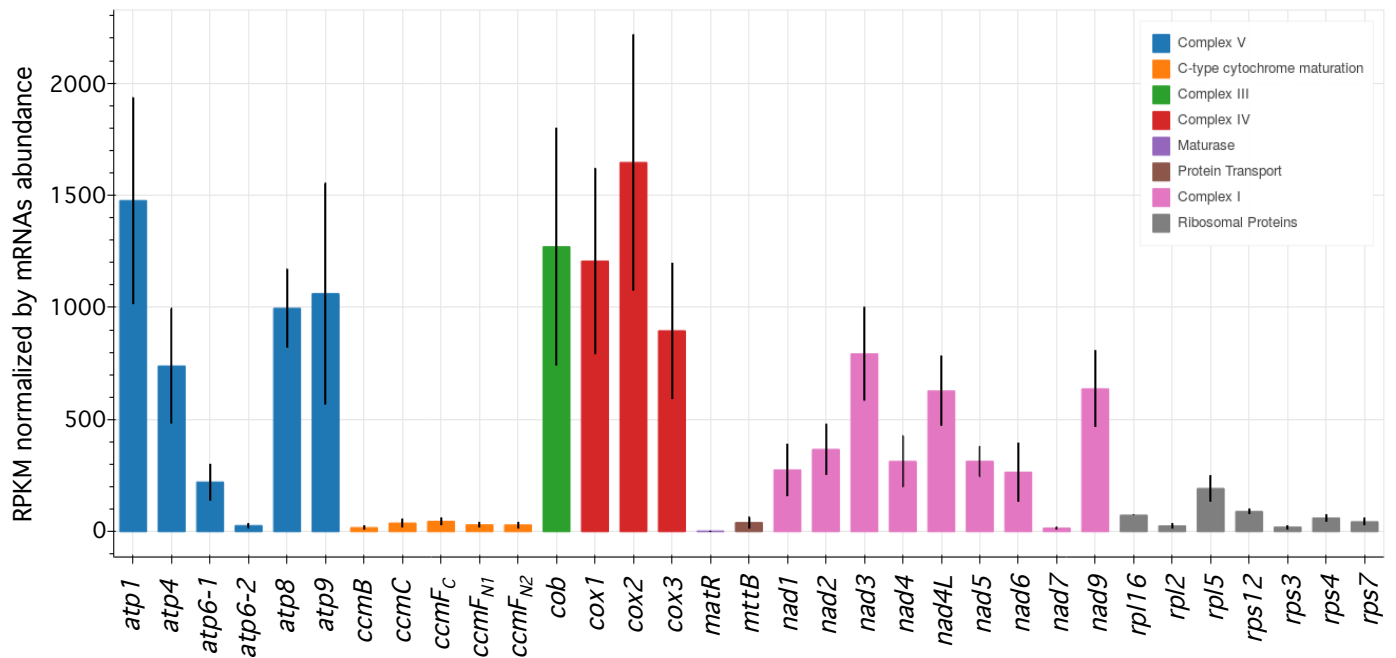


Figure S6: RPF coverage of mitochondrial mRNAs in the *Arabidopsis mt/l1* mutant. RPF densities normalized by both mRNA length and abundance are shown. Mitochondrial mRNAs are indicated and color-coded according to the respiratory complex or the functional category to which they belong. Means \pm SE (n = 2).

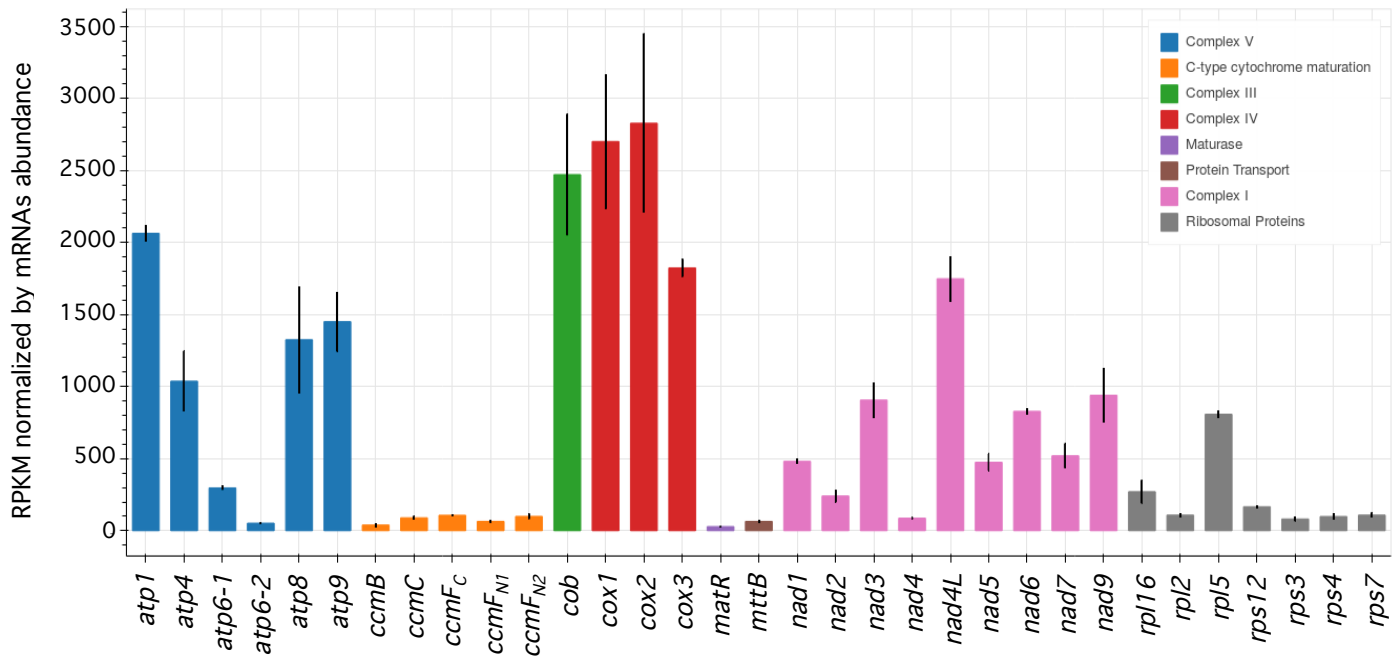


Figure S7: RPF coverage of mitochondrial mRNAs in the Arabidopsis *mts1* mutant. RPF densities normalized by both mRNA length and abundance are shown. Mitochondrial mRNAs are indicated and color-coded according to the respiratory complex or the functional category to which they belong. Means \pm SE (n = 2).

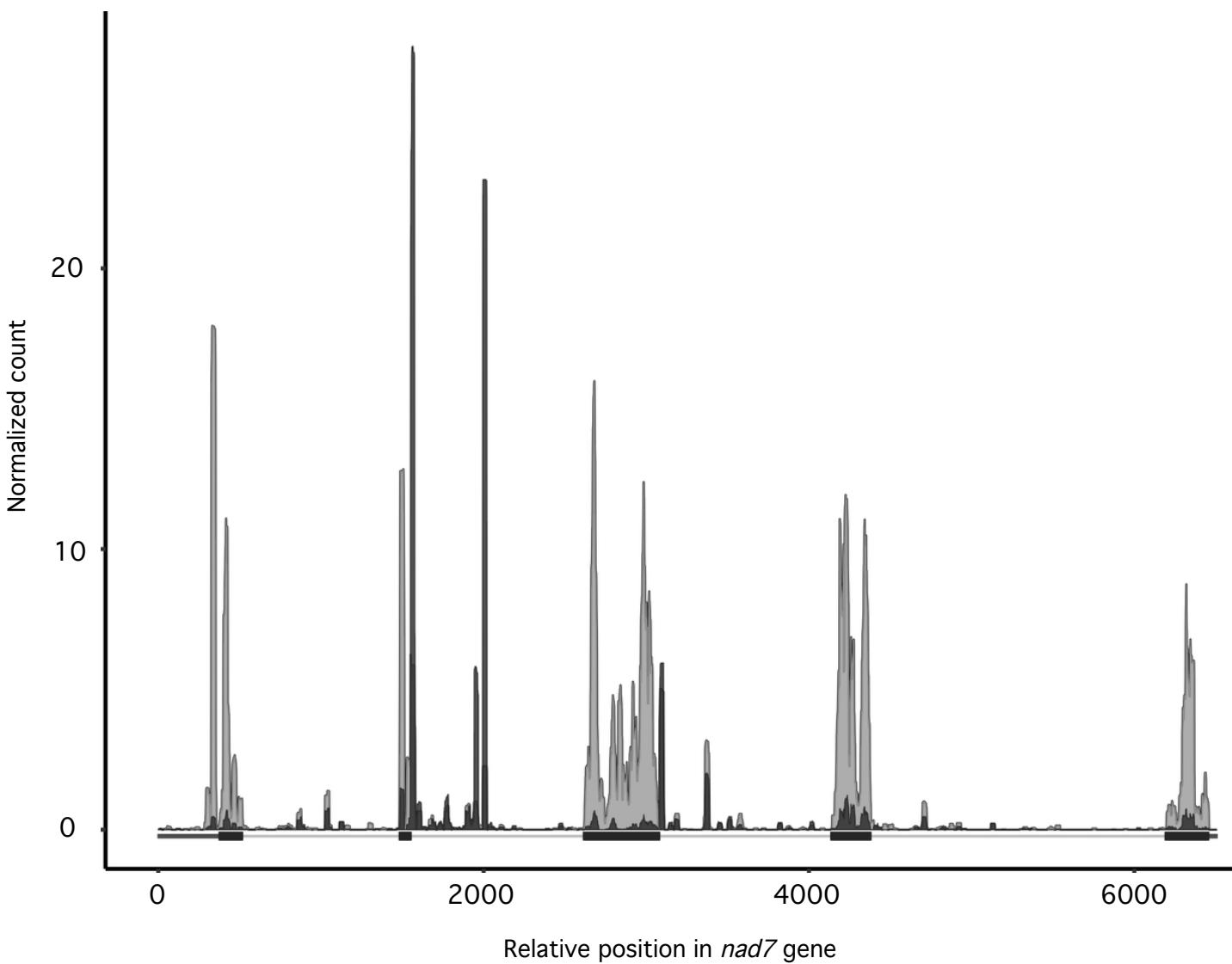


Figure S8: RPF coverage along the *nad7* mRNA in Col-0 (grey) and *mt/1* (black) plants. Ribosome footprint coverage in Col-0 is shown in light grey, coverage in *mt/1* is in black.